united nations educational, scientific and cultural organization

international atomic energy agency

the
abdus salam
international centre for theoretical physics

SMR 1331/25

AUTUMN COLLEGE ON PLASMA PHYSICS

8 October - 2 November 2001

The α–effect and Current Drive Using Electron Bernstein Waves in the RFP

Cary Forest

Dept. of Physics, University of Wisconsin, U.S.A.

strada costiera, 11 - 34014 trieste italy - tel. +39 040 2240111 fax +39 040 224163 - sci_info@ictp.trieste.it - www.ictp.trieste.it

Outline

- The α effect in the RFP-components of dynamo physics
- RF heating and current in an RFP
  - Impact of current profile modification on performance
  - Magnetic geometry and dielectric properties
- Electron Bernstein Waves
  - Propagation, absorption and current drive
  - Coupling
- Emission measurements
  - Black body levels of emission observed
- Coupling measurements
  - Agreement with waveguide coupling theory
- Plans

The α effect in the Reversed Field Pinch

- The α-effect predicted from mean-field electrodynamics plays an important role in the RFP
  - Predicts generation of current in direction of pre-existing magnetic field from fluctuations
- Global kink-tearing modes provide fluctuating magnetic and velocity fields (driven by gradients in current density)
- α effect generate toroidal magnetic flux from poloidal magnetic field
- Not a dynamo since free energy source is gradients in magnetic field energy
  - Referred to as "RFP dynamo-effect"

The standard RFP current profile is sustained by a toroidal electric field and MHD fluctuation driven currents

- toroidal electric field drives toroidal current in core
- peaked current profile is unstable to tearing modes

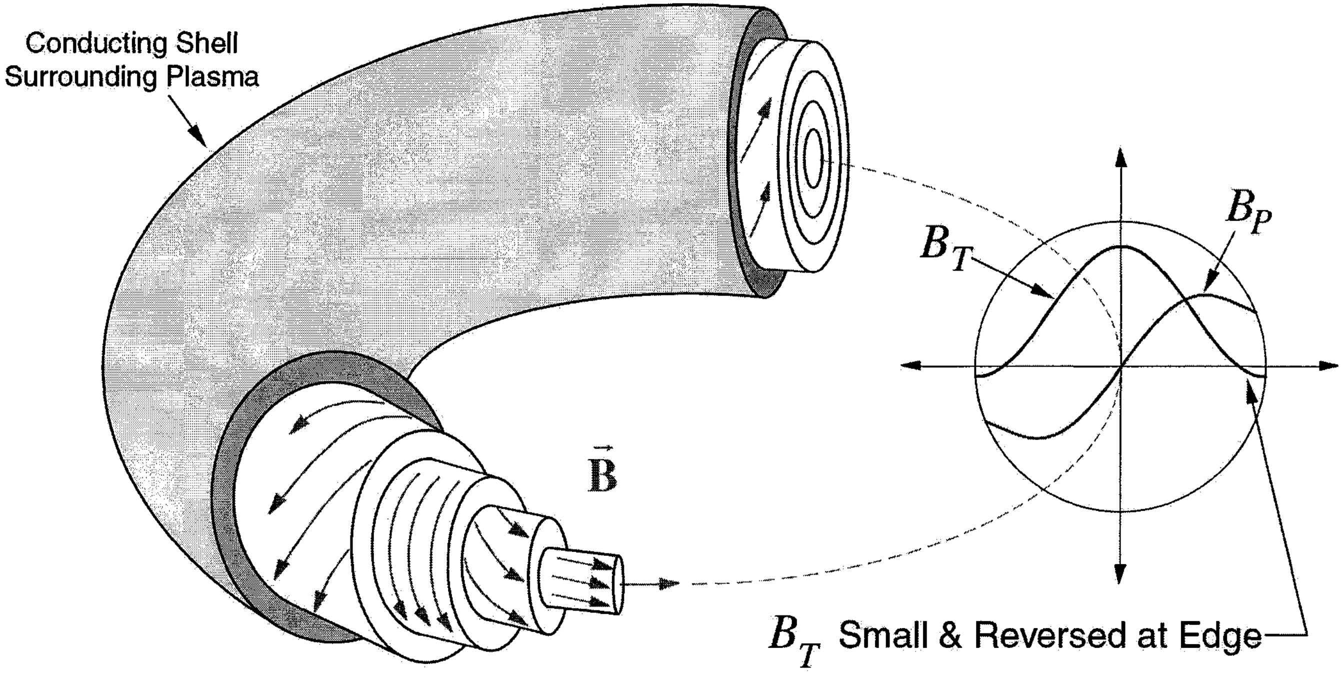

Tearing modes drive poloidal current in the edge and suppress current in core

- broad spectrum of tearing mode are driven by gradients in $\lambda = J_{\|}/B$
- current profile driven by MHD towards a marginally stable current profile (flat λ)
- Island overlap causes stochastic magnetic transport in core

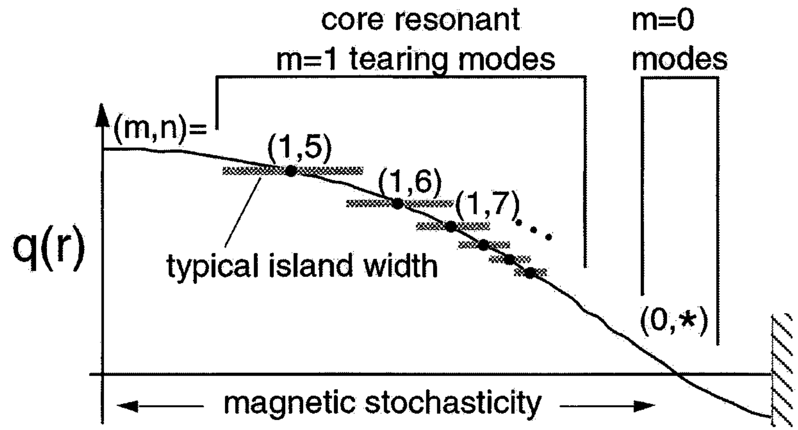

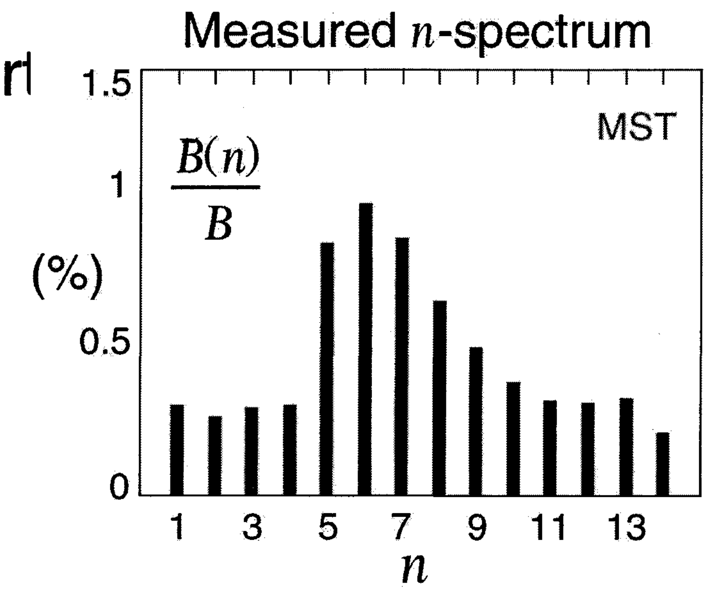

An α-effect is needed to sustain the RFP equilibrium (Cowling's theorem applied to the RFP)

Assume axisymmetry and a simple Ohm's law ($\mathbf{J} = \sigma \mathbf{E}$). Now consider current at reversal surface (surface where $B_\phi = 0$)

$$J_\theta = -\frac{\partial B_\phi}{\partial r} \neq 0$$

but

$$\begin{aligned} \frac{d\Phi}{dt} &= -E_\theta 2\pi r \\ &= -\frac{J_\theta}{\sigma} 2\pi r \\ &= \frac{1}{\mu_0 \sigma} \frac{\partial B_\phi}{\partial r} \\ &\leq 0, \end{aligned}$$

thus no steady-state field reversal is compatable with simple Ohm's law.

An α-effect is needed to sustain the RFP equilibrium (continued)

Now consider an Ohm's law of the form $(\mathbf{J} = \sigma\mathbf{E} + \alpha\mathbf{B})$.
Now,

$$\begin{aligned}
\frac{d\Phi}{dt} &= -E_\theta 2\pi r \\
&= \left(-\frac{J_\theta}{\sigma} + \alpha B_\theta\right) 2\pi r \\
&= \frac{2\pi r}{\mu_0 \sigma}\frac{\partial B_\phi}{\partial r} + 2\pi r \alpha B_\theta .
\end{aligned}$$

Now, steady state is possible if

$$\frac{\partial B_\phi}{\partial r} = \mu_0 \sigma \alpha B_\theta .$$

(Recall Taylor state $\nabla \times \mathbf{B} = \lambda \mathbf{B}$)

Toroidal flux for RFP equilibrium is periodically regenerated in discrete sawteeth events

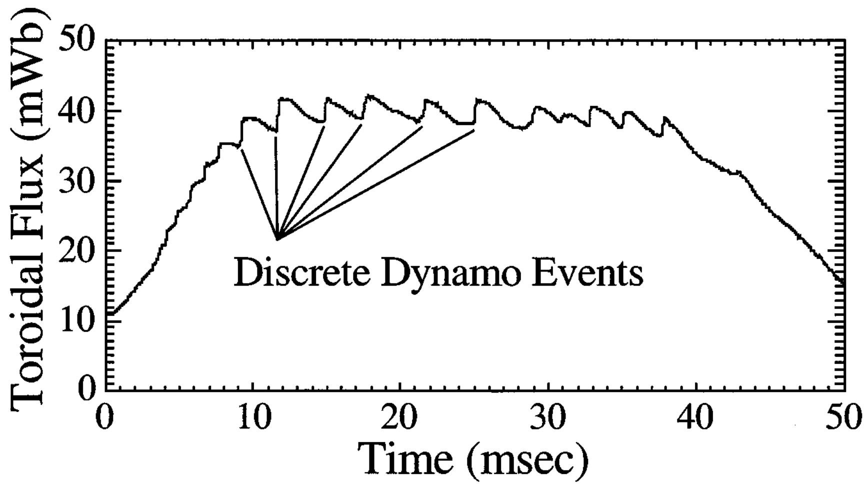

- Reversed field equilibrium can be sustained for many resistive diffusion times
- Toroidal flux follows current
- Theory of relaxation is beyond scope of this talk, but it involves

Velocity and magnetic field fluctuations can be measured to estimate motional EMF from tearing modes

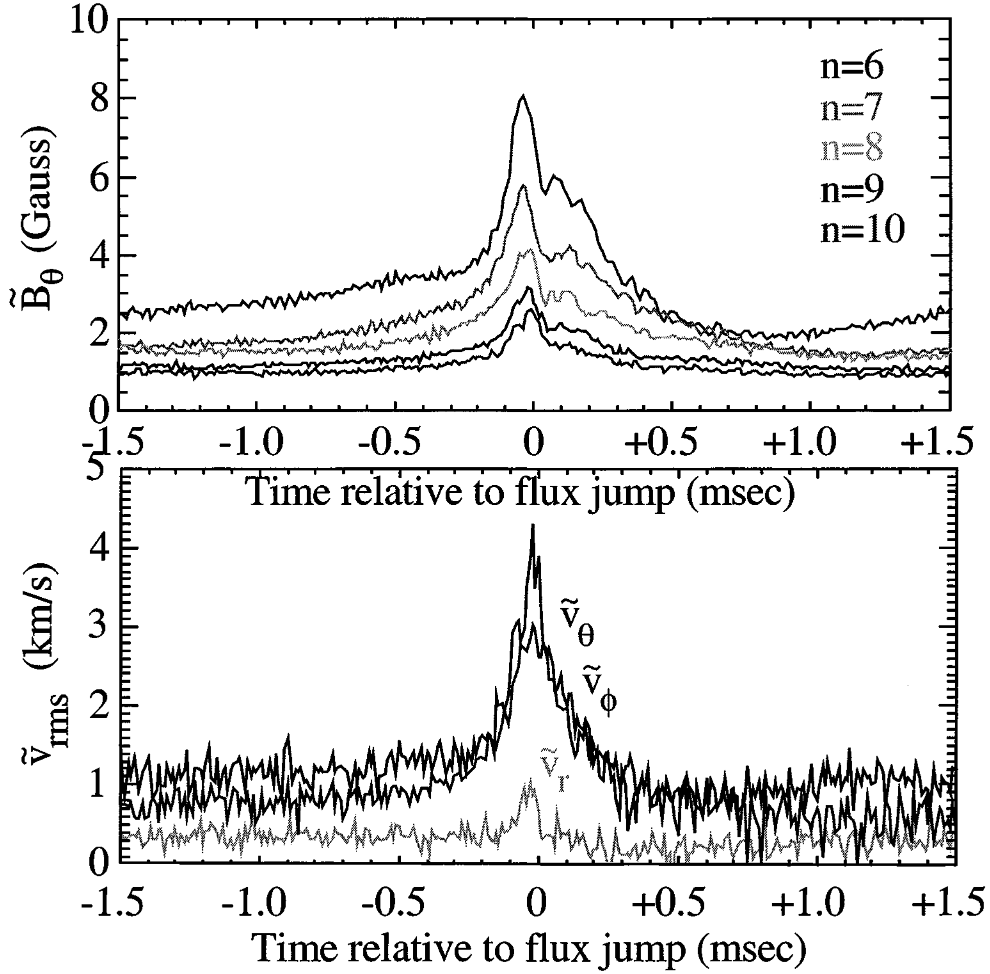

Mean-field EMF from tearing modes regenerate toroidal flux

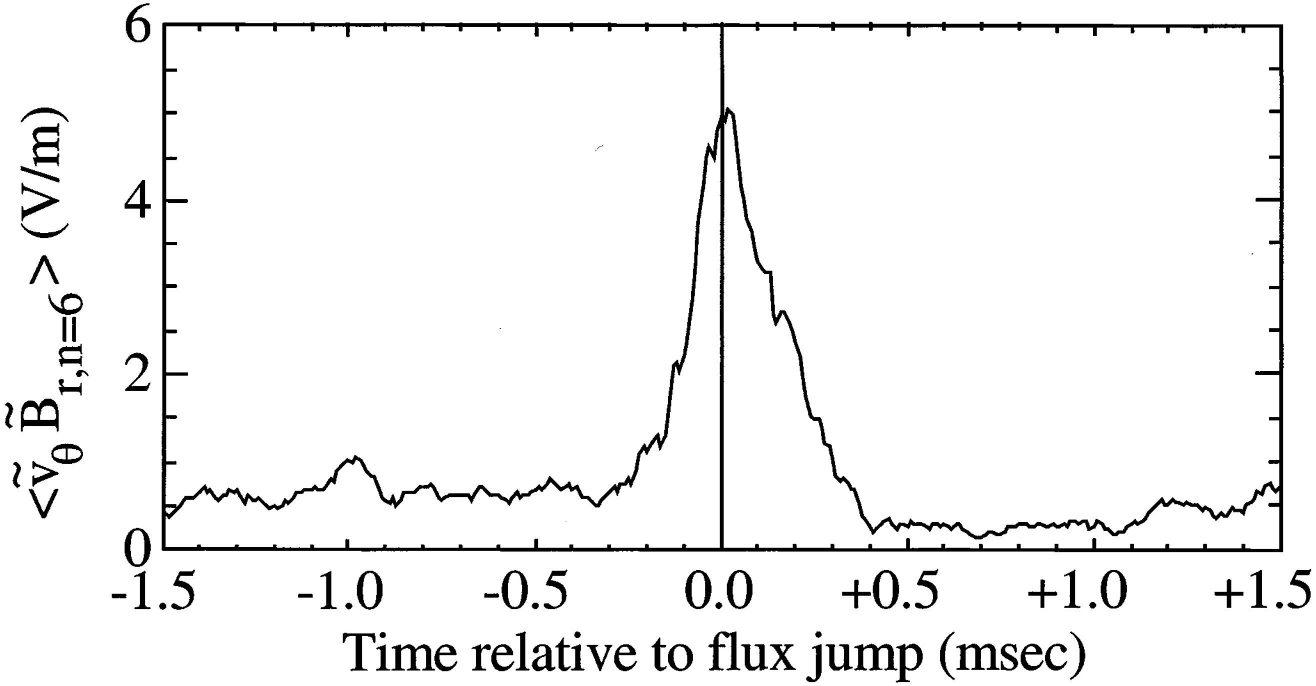

Hypothesis:

The RFP's poor confinement is a result of the misalignment of inductive CD profile and tearing mode stable current profiles.

By non-inductively sustaining a current profile which is linearly stable to all tearing modes, the confinement in the RFP will improve.

$\longrightarrow$ Produce a non-inductively driven Taylor-State

MHD simulations indicate partial current drive in the edge region of the RFP can reduce magnetic fluctuations

$$\frac{\partial \mathbf{A}}{\partial t} + \frac{F_a \hat{\mathbf{b}}}{ne} = \mathbf{V} \times \mathbf{B} - \eta \mathbf{J}$$

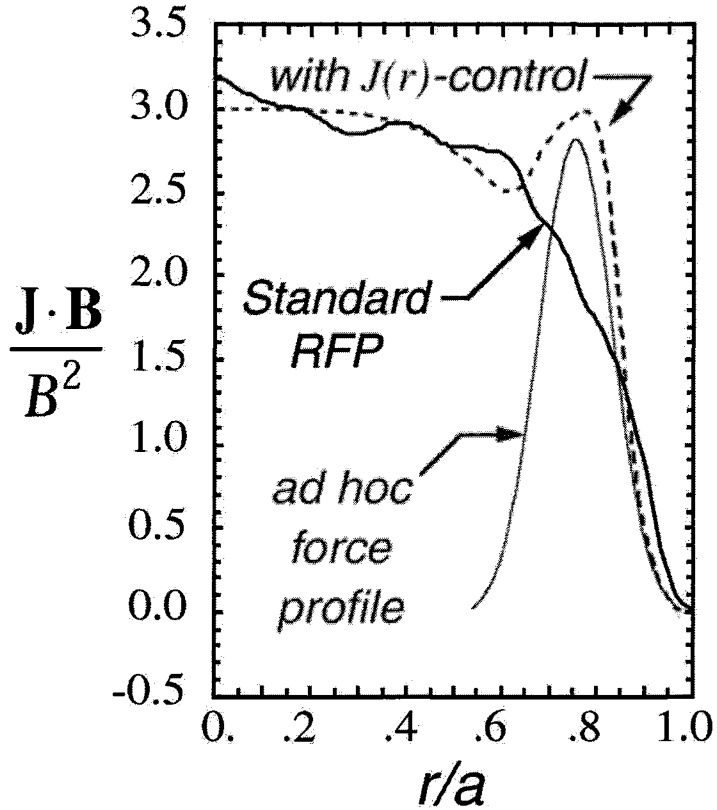

Nonlinear, 3D resistive MHD computation

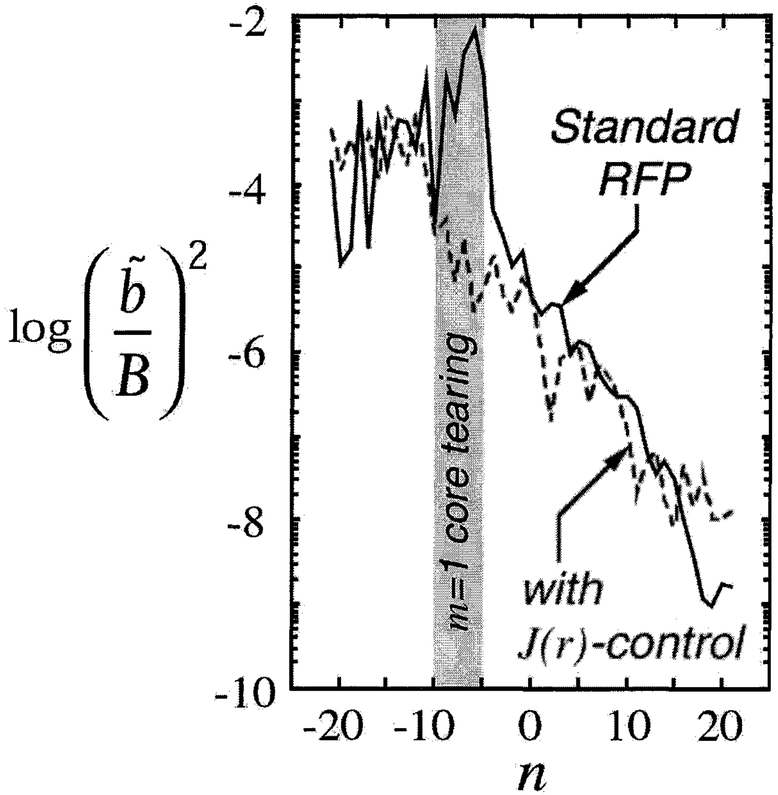

Current drive can heal flux surfaces

Standard RFP

Stochastic Field

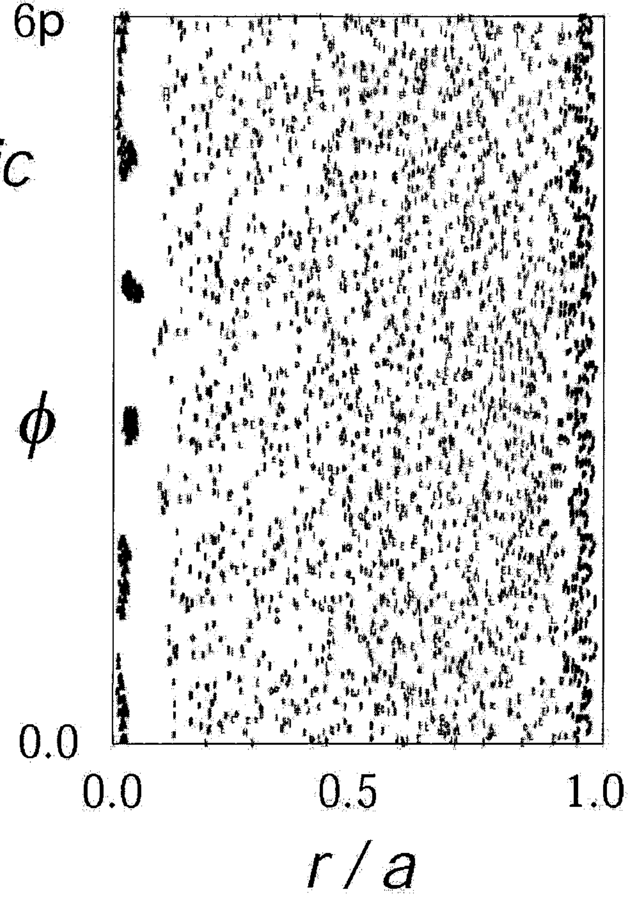

RFP with J(r)-Control

Closed Flux Surfaces

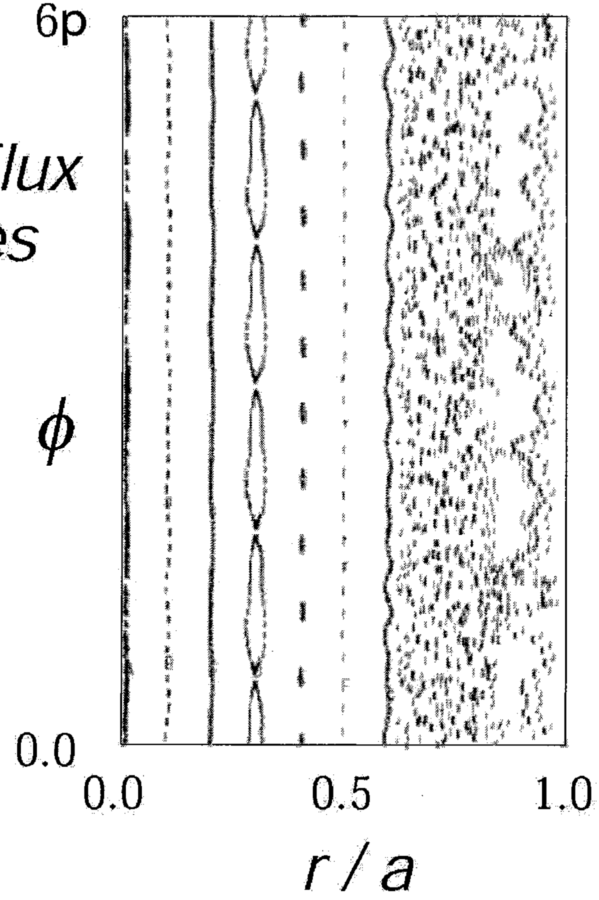

PPCD: inductive electric field programming results reduction of magnetic fluctuations (for 10 ms)

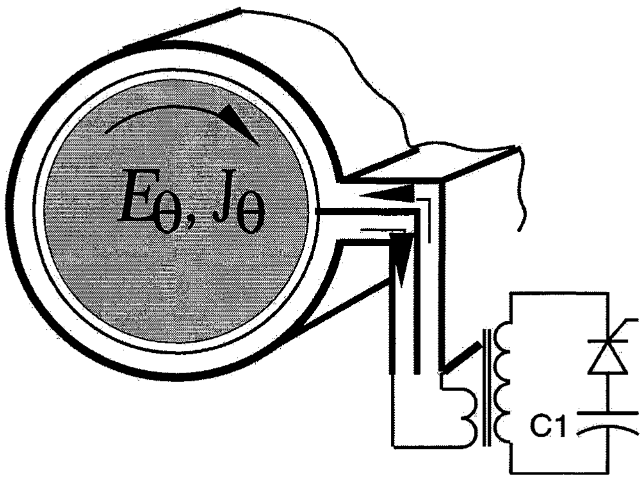

Pulsed Poloidal Current Drive

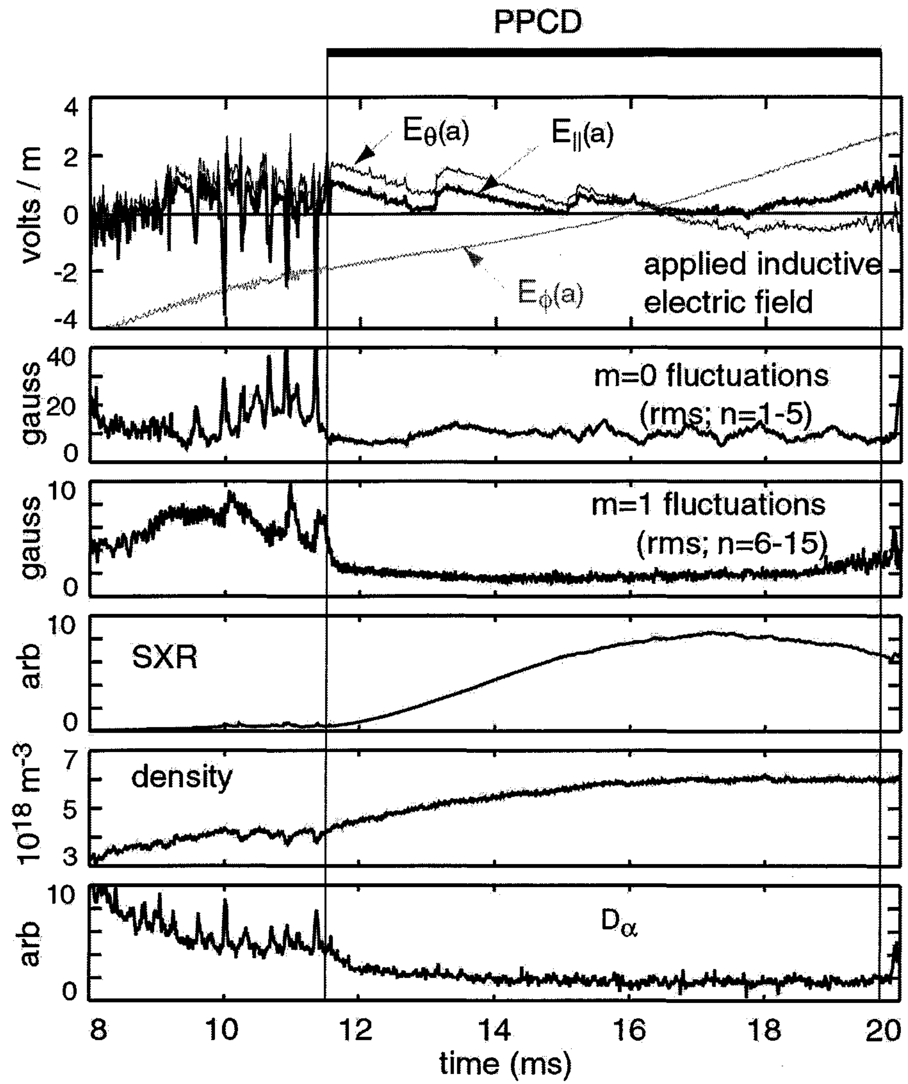

Electron energy transport is improved during PPCD: excellent target plasmas for RF current drive

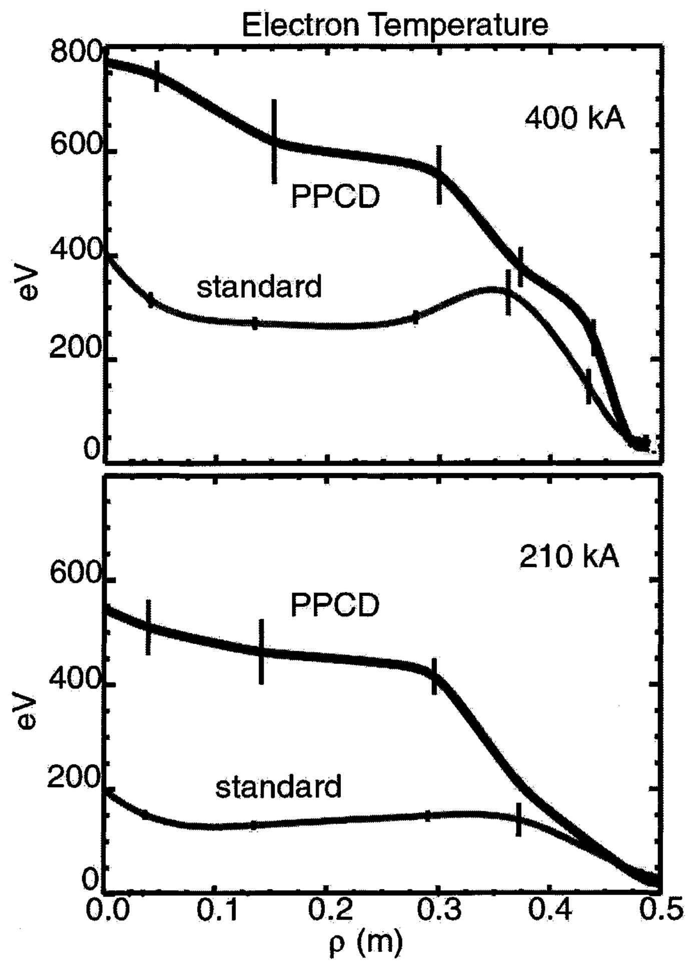

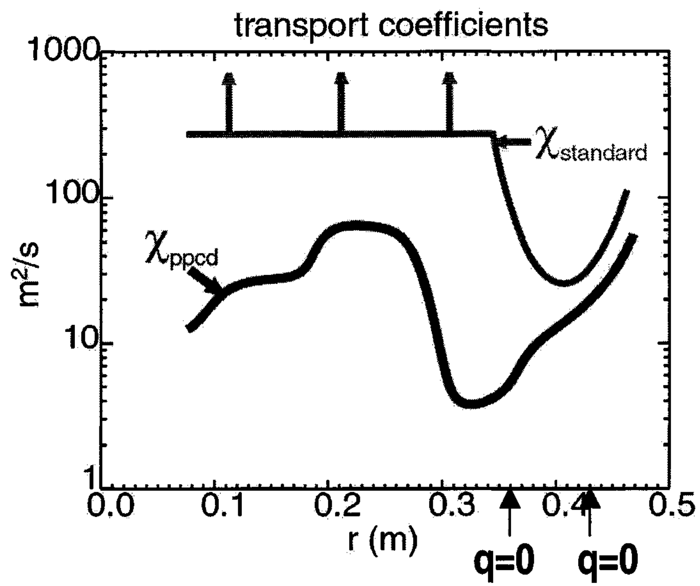

- χ_e drops by factor of 10 during PPCD
- τ_E=10 ms, n_e = 0.5-1.0 $\times$ 10^{13} cm^{-3}
  P < 1 MW

PPCD shows good fast electron confinement: runaway electrons are present

- Pulse height analysis of PPCD plasmas show 100 keV electrons
- RF generated tail of the electron distribution function can be confined!
- Fokker-Planck Modeling shows diffusion coefficient of $5 m^2/s$, measured Z_{eff} matches data well, even with Diffusion=$0 m^2/s$, Z_{eff} ~3 needed

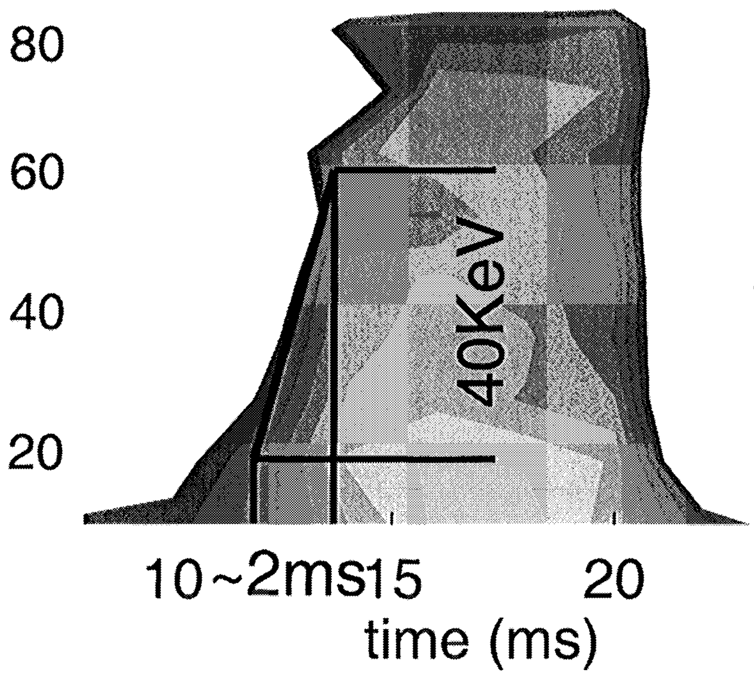

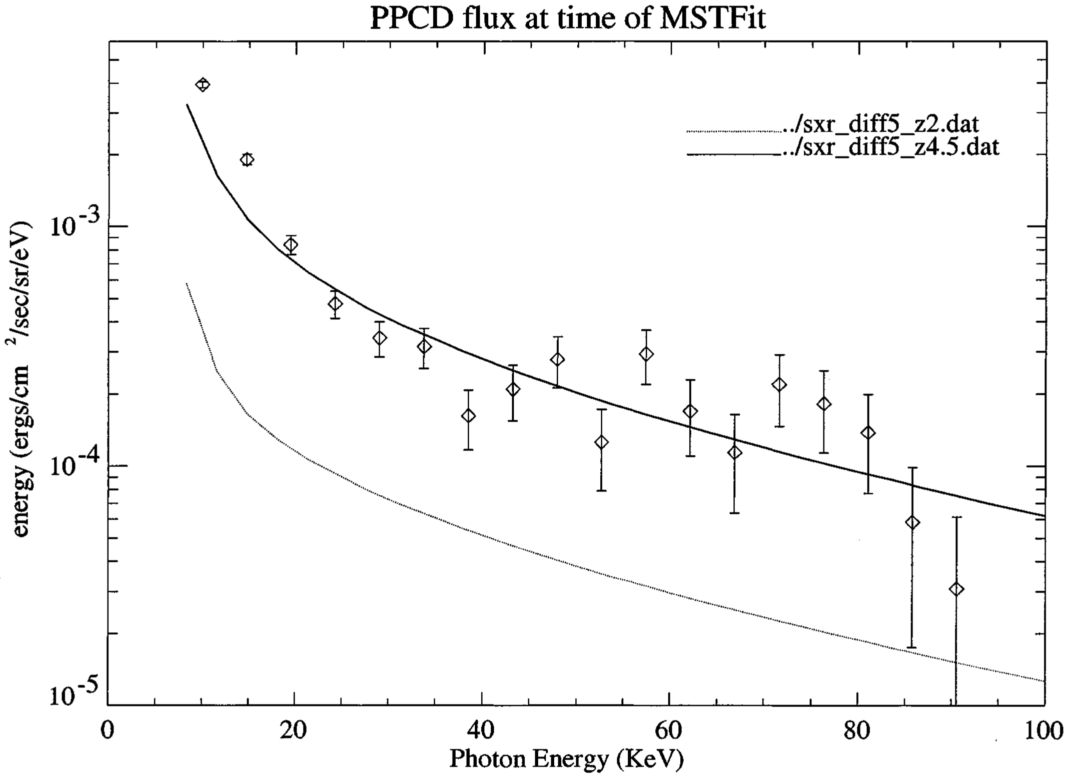

MST plasmas are over-dense

- High dielectric constant

$$\frac{\omega_{pe}}{\Omega_{ce}} > 5$$

- Conventional electromagnetic waves in the electron cyclotron range of frequencies do not propagate
- LH wave accessibility is limited

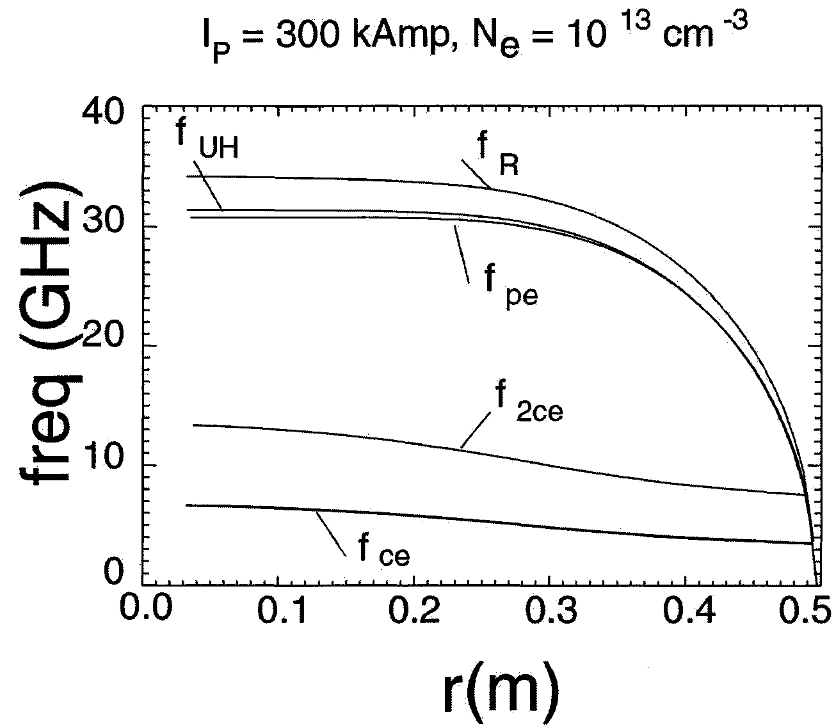

What type of waves might propagate for these parameters in the ECRF

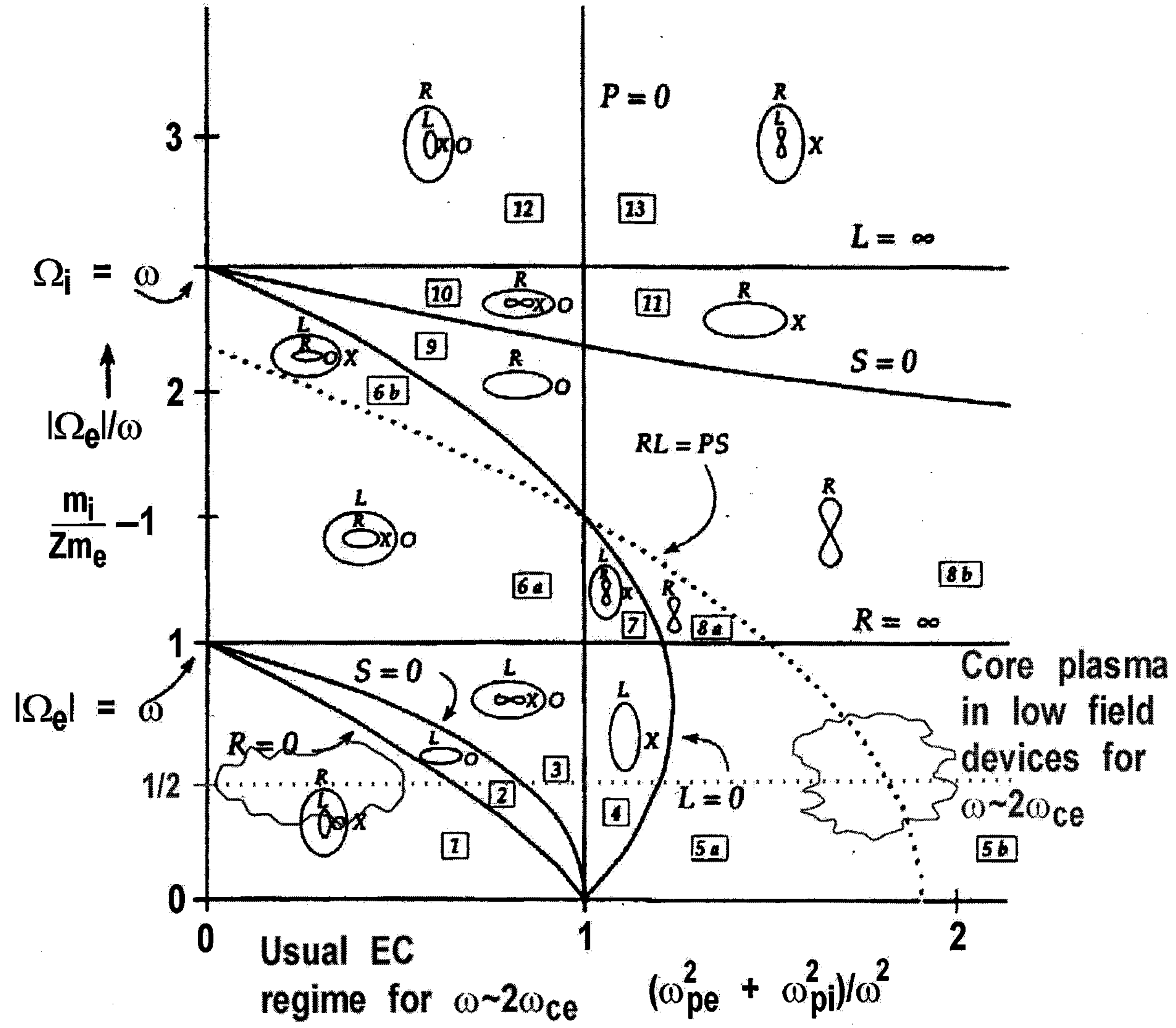

The EBW propagates when the plasma is overdense

- Hot plasma wave
- Wavelength of order ρ_e
- Propagates nearly perpendicular to magnetic field
- Primarily electrostatic

Typical EBW Dispersion Curves

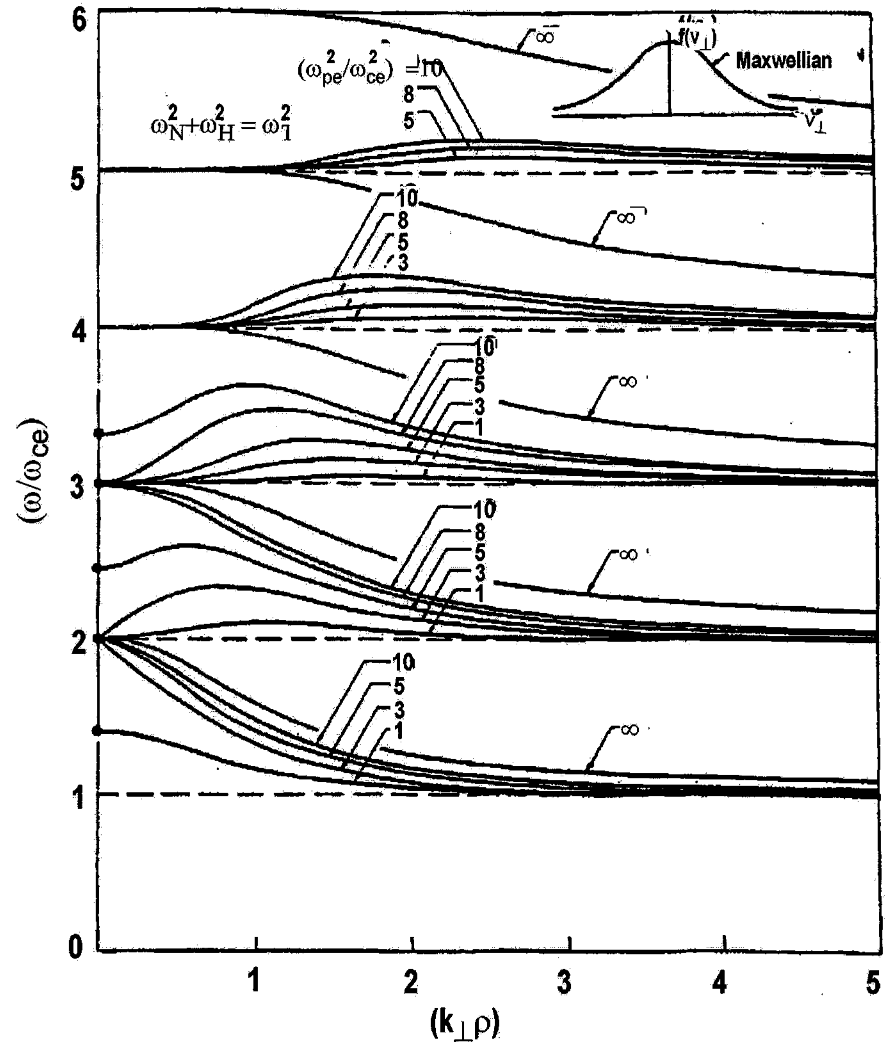

$$\epsilon(\omega,\mathbf{k}) = 1 - \frac{2\omega_{pe}^2}{k^2 v_{Te}^2}\sum_{n=-\infty}^{n=\infty}\left(\frac{n\Omega_{ce}}{\omega-n\Omega_{ce}} + \frac{\omega}{\omega-n\Omega_{ce}}\frac{Z'(\xi_n)}{2}\right)e^{-\lambda}I_n(\lambda) = 0$$

Hot plasma dispersion can be evaluated numerically

Assuming a maxwellian distribution function $f(v) = \left(\frac{m}{2\pi kT}\right)^{3/2} \exp \frac{-mv^2}{2kT}$, the hot plasma dielectric tensor is

$$\mathrm{K} = 1 + Xe^{-\lambda} \sum_{n=-\infty}^{\infty} \begin{pmatrix} \frac{n^2}{\lambda} I_n A_n & -in\left(I_n - I_n'\right) A_n & \frac{n}{\lambda} N_\perp I_n B_n / Y \\ in\left(I_n - I_n'\right) A_n & \left(\frac{n^2}{\lambda} I_n + 2\lambda\left(I_n - I_n'\right)\right) A_n & iN_\perp\left(I_n - I_n'\right) B_n / Y \\ -\frac{n}{\lambda} N_\perp I_n B_n / Y & -iN_\perp\left(I_n - I_n'\right) B_n / Y & 2\frac{(1-nY)}{N_\| \beta^2} I_n B_n \end{pmatrix}, \tag{1}$$

where $\lambda = \frac{k_\perp^2 kT}{m\Omega^2} = \frac{N_\perp^2 \beta^2}{2Y^2}$, $X = \frac{\omega_{pe}^2}{\omega^2}$, $Y = \frac{\Omega}{\omega}$, $\beta^2 = \frac{2kT}{mc^2}$, $N_\perp = \frac{k_\perp c}{\omega}$. Here, the functions

$$\begin{aligned} A_n &= \frac{Z\left(\xi_n\right)}{N_\| \beta}, \\ B_n &= \frac{1 + \xi_n Z\left(\xi_n\right)}{N_\|}, \\ \xi_n &= \frac{1 - nY}{N_\| \beta}, \end{aligned}$$

$I_n = I_n(\lambda)$ is the modified bessel function, and $Z(\xi)$ is the plasma dispersion function.

T.H. Stix *Waves in Plasmas*, AIP (1992)

Hot plasma dispersion (continued)

Solve wave equation

$$\boldsymbol{N} \times (\boldsymbol{N} \times \boldsymbol{E}) + \boldsymbol{K} \cdot \boldsymbol{E} = \boldsymbol{0}, \tag{1}$$

which in matrix form is

$$\begin{pmatrix} K_{xx} - N_{\|}^2 & K_{xy} & K_{xz} + N_{\perp}N_{\|} \\ K_{yx} & K_{yy} - N_{\perp}^2 - N_{\|}^2 & K_{yz} \\ K_{zx} + N_{\perp}N_{\|} & K_{zy} & K_{zz} - N_{\perp}^2 \end{pmatrix} \begin{pmatrix} E_x \\ E_y \\ E_z \end{pmatrix} = 0, \tag{2}$$

Functionally, this is specified as

$$D(X, Y, \beta, N_{\perp}, N_{\|}) = 0 = \begin{vmatrix} K_{xx} - N_{\|}^2 & K_{xy} & K_{xz} + N_{\perp}N_{\|} \\ K_{yx} & K_{yy} - N_{\perp}^2 - N_{\|}^2 & K_{yz} \\ K_{zx} + N_{\perp}N_{\|} & K_{zy} & K_{zz} - N_{\perp}^2 \end{vmatrix} \tag{3}$$

Solve for $N_{\perp}$, given X, Y, β and $N_{\|}$. Dispersion found from Re$D(N_{\perp,r}) = 0$, where $N_{\perp,r}$ is the real part of N; damping found from

$$N_{\perp,i} = -\frac{D_I(N_{\perp,r})}{\frac{\partial D_R}{\partial N_{\perp}}} \tag{4}$$

Ray Tracing in general toroidal geometry

Once root is found, it can be followed with Hamiltonian ray tracing equations to solve for the ray trajectories of the waves:

$$\begin{aligned}
\frac{\partial z}{\partial t} &= -\frac{c}{\omega}\frac{\partial D/\partial N_z}{\partial D/\partial\omega};\ \frac{\partial N_z}{\partial t} = \frac{c}{\omega}\frac{\partial D/\partial z}{\partial D/\partial\omega};\\
\frac{\partial r}{\partial t} &= -\frac{c}{\omega}\frac{\partial D/\partial N_r}{\partial D/\partial\omega};\ \frac{\partial N_r}{\partial t} = \frac{c}{\omega}\frac{\partial D/\partial r}{\partial D/\partial\omega};\\
\frac{\partial \phi}{\partial t} &= -\frac{c}{\omega}\frac{\partial D/\partial m}{\partial D/\partial\omega};\ \frac{\partial m}{\partial t} = \frac{c}{\omega}\frac{\partial D/\partial \phi}{\partial D/\partial\omega}.
\end{aligned}$$

The spatial derivatives are computed from equilibrium quantites and chain rule, ie.

$$\begin{aligned}
\frac{\partial D}{\partial r} &= \frac{\partial D}{\partial X}\frac{\partial X}{\partial r} + \frac{\partial D}{\partial Y}\frac{\partial Y}{\partial r} + \frac{\partial D}{\partial \beta}\frac{\partial \beta}{\partial r}\\
\frac{\partial D}{\partial z} &= \frac{\partial D}{\partial X}\frac{\partial X}{\partial z} + \frac{\partial D}{\partial Y}\frac{\partial Y}{\partial z} + \frac{\partial D}{\partial \beta}\frac{\partial \beta}{\partial z}\\
\frac{\partial D}{\partial \phi} &= 0
\end{aligned}$$

Toroidal equilibrium is used for calculation of magnetic field.

Numerical study of EBW propagation and absorption has been carried out using GENRAY and CQL3D

- Full hot, non-relativistic dispersion solver
- Absorption is complete (nearly infinite optical thickness)

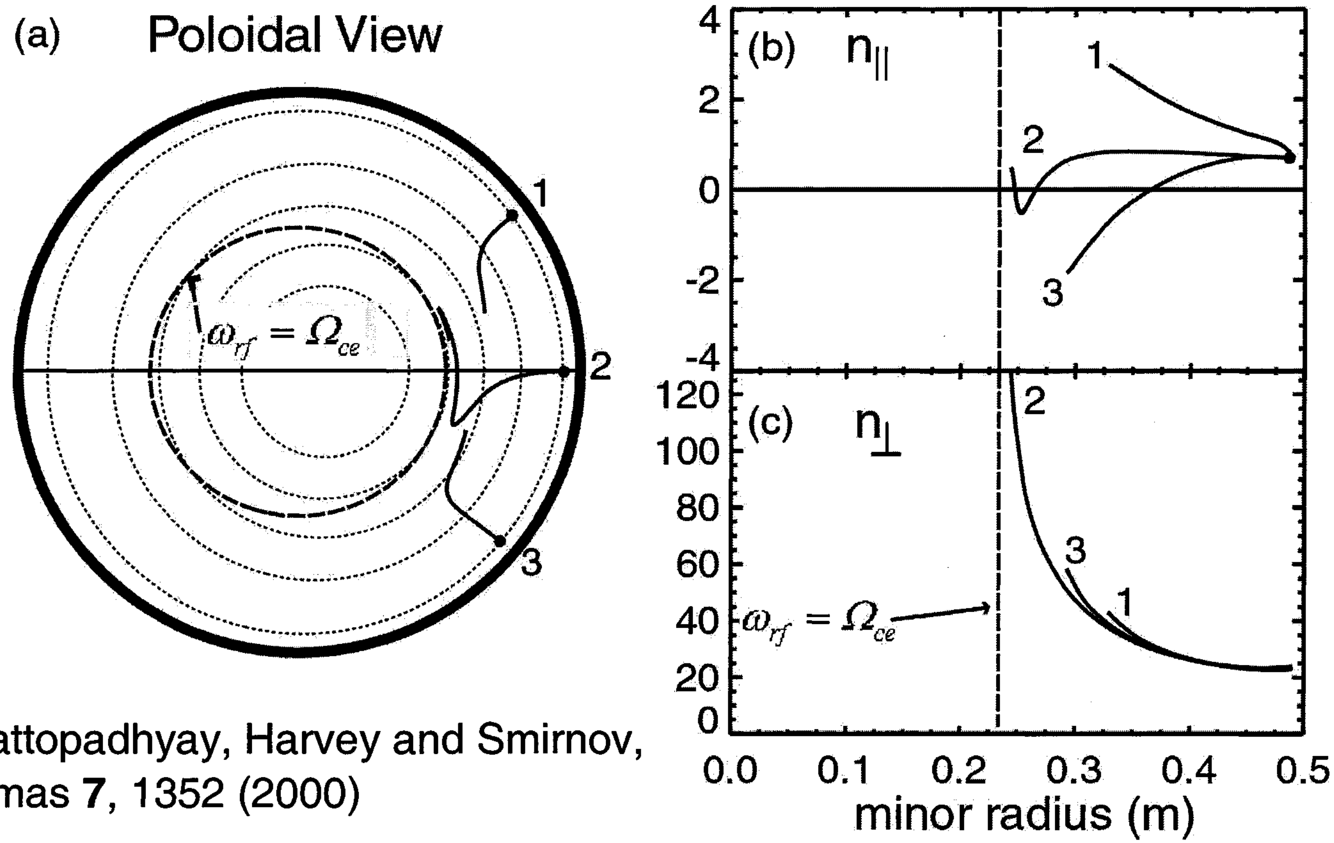

Forest, Chattopadhyay, Harvey and Smirnov, Phys. Plasmas **7**, 1352 (2000)

$N_{\parallel}$ up-shift and direction of CD can be controlled by poloidal launch position

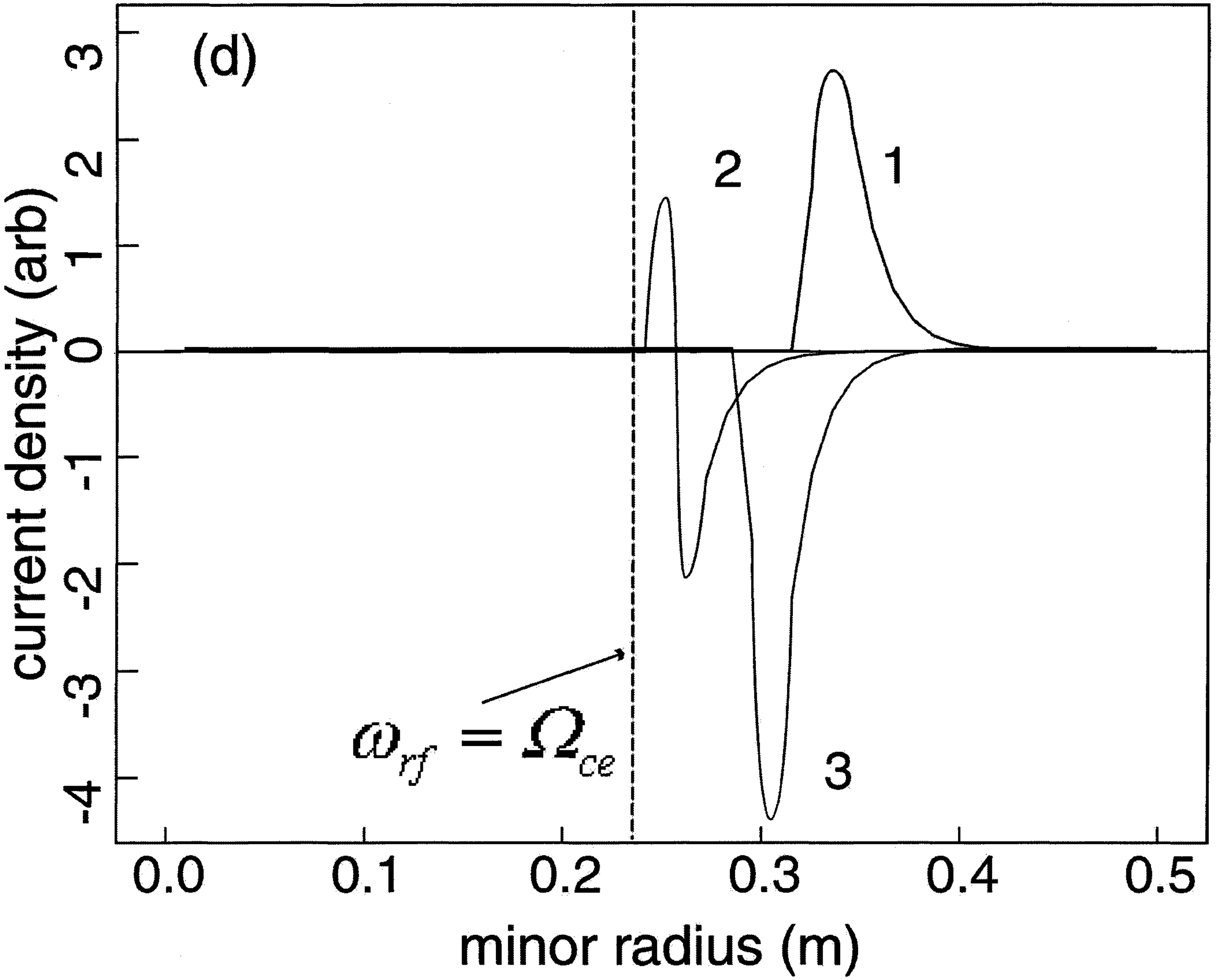

RFP physics is similar to ST physics (ECH characteristics of Pegasus are similar to MST)

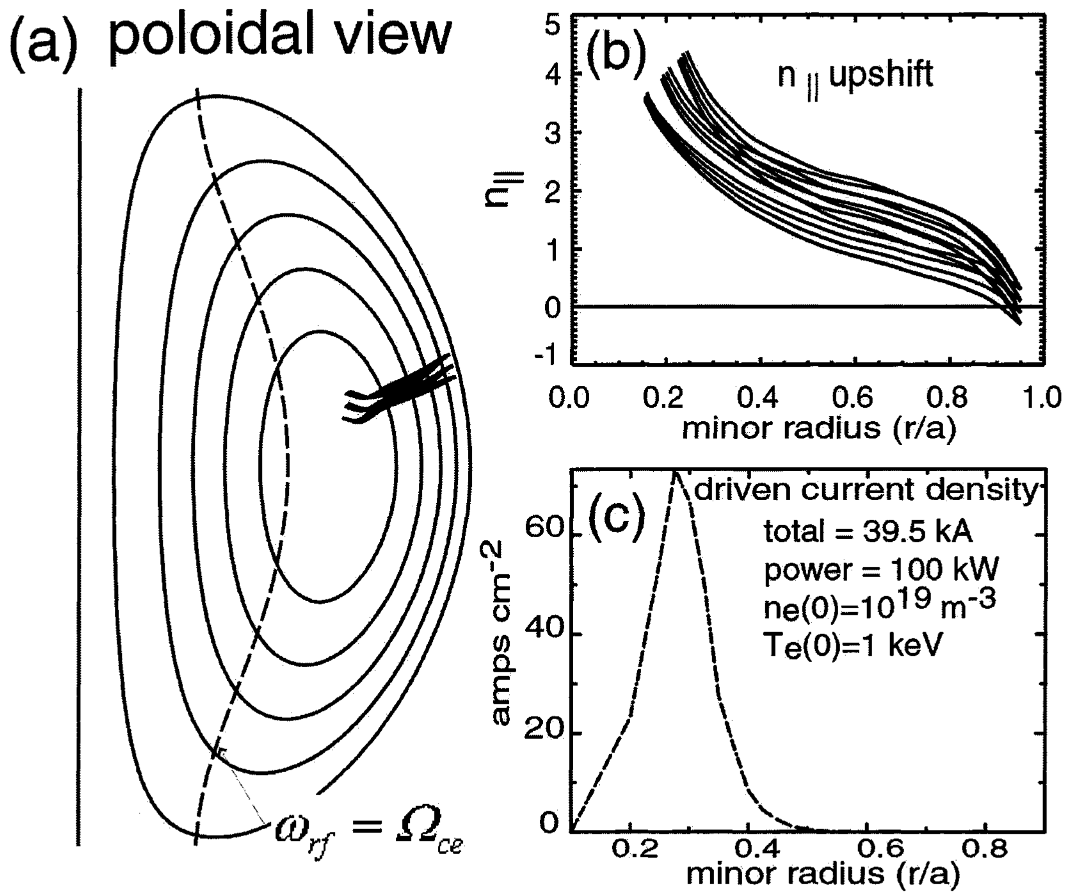

Forest and Ono, Bull. Am. Phys. Soc. **35**, 2057 (1990)

Forest, Chattopadhyay, Harvey and Smirnov, Phys. Plasmas **7**, 1352 (2000)

Current drive is computed from solution of Fokker-Planck Equation (CQL3D)

- Hot plasma dispersion is non-relativistic
- CQL3D uses non-relativistic polarizations but fully relativistic Fokker-Plank treatment
- Wave diffusion determined from electric field (from ray tracing code)

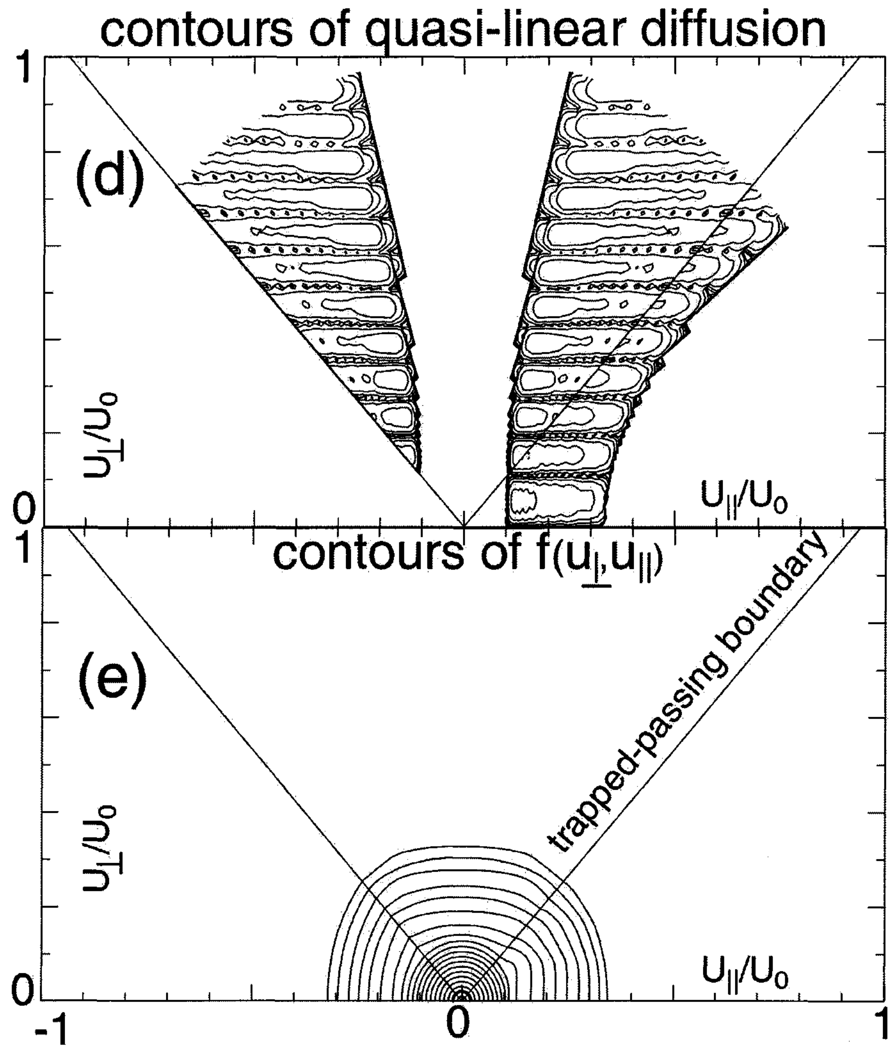

History of Coupling

- Early theory
  - Mode conversion theory Stix (Phys. Rev. Lett, 1966)
    - Couple to the EBW using an X mode launched from the high field side
  - Hot plasma waves (Bernstein)
- Early experiments (~1970)
  - Observation of the EBW (Leuterer, Stenzel, Armstrong)
  - Non-linear effects and heating (Porkolab)
- OXB mode conversion identified (1972)
  - Pioneering work by Preinhalter and Kopecky, 1972
  - Later work by Batchelor and Goldfinger
- Tunneling through XB (Sugai)
- Demonstration of OXB on Wendelstein 7-AS
  - Heating, emission (Laqua, et al 1996, 1998)
- Recognized as possible heating source for STs
  - Forest (1990), Ram and Bers (1998)
- Ongoing research on STs and RFPs

X-mode incident on upper-hybrid resonance from high field or high density side smoothly mode converts into EBW: classic mode-conversion problem

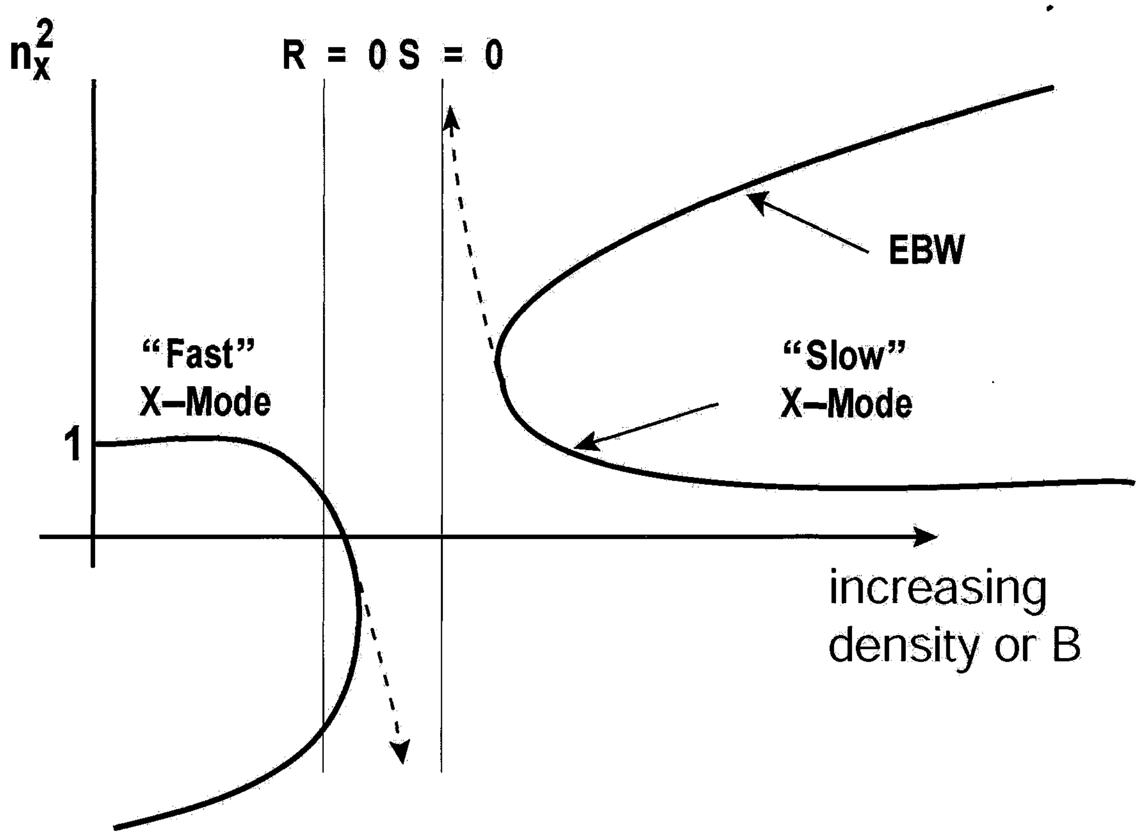

T.H. Stix, Phys. Rev. Lett. **15** 878 (1965)

Launching the EBW with high field side X mode for inside launch 60 GHz ECH on DIII-D

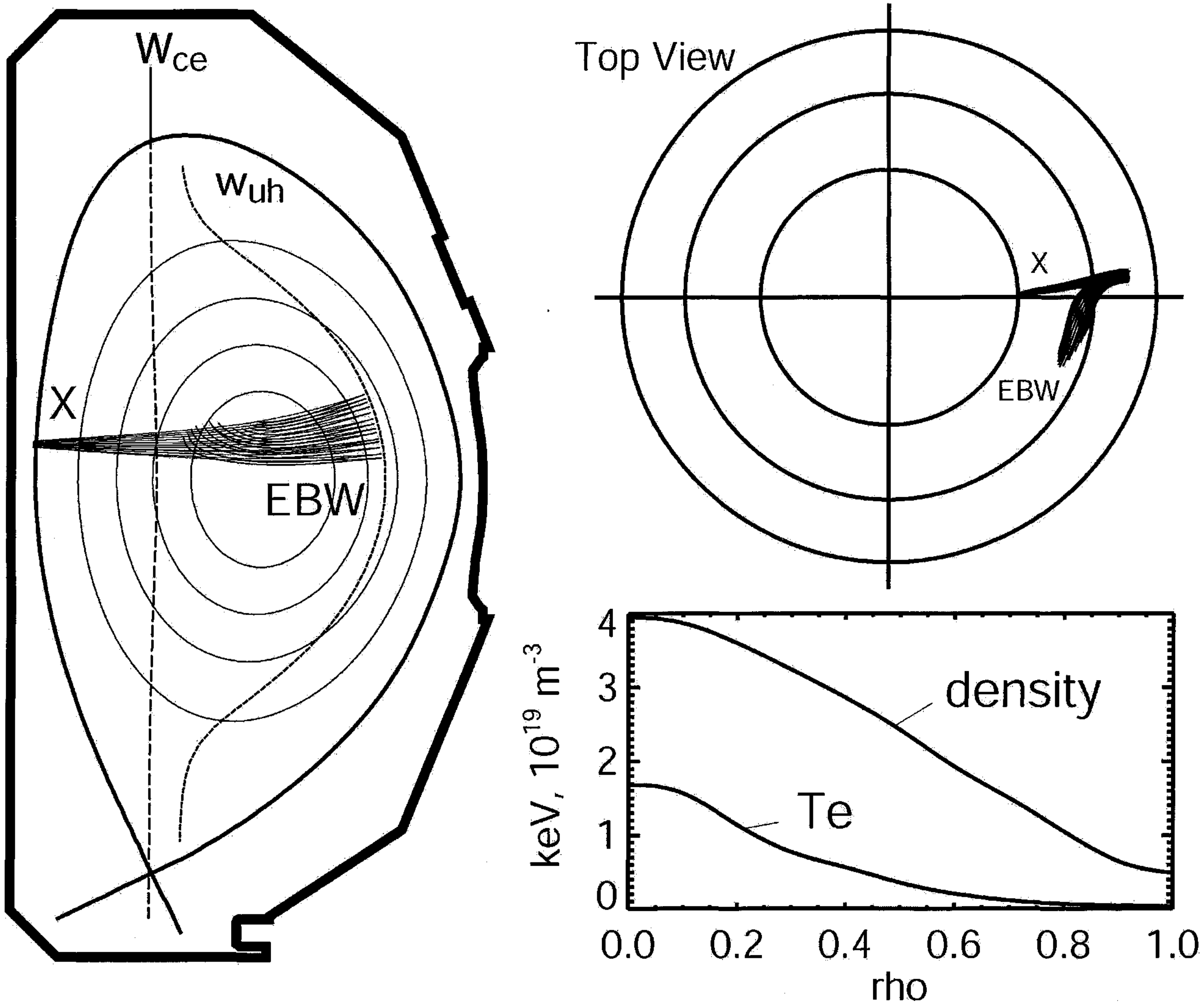

EBW may play a role in understanding the "Heat-Pinch" results on DIII-D

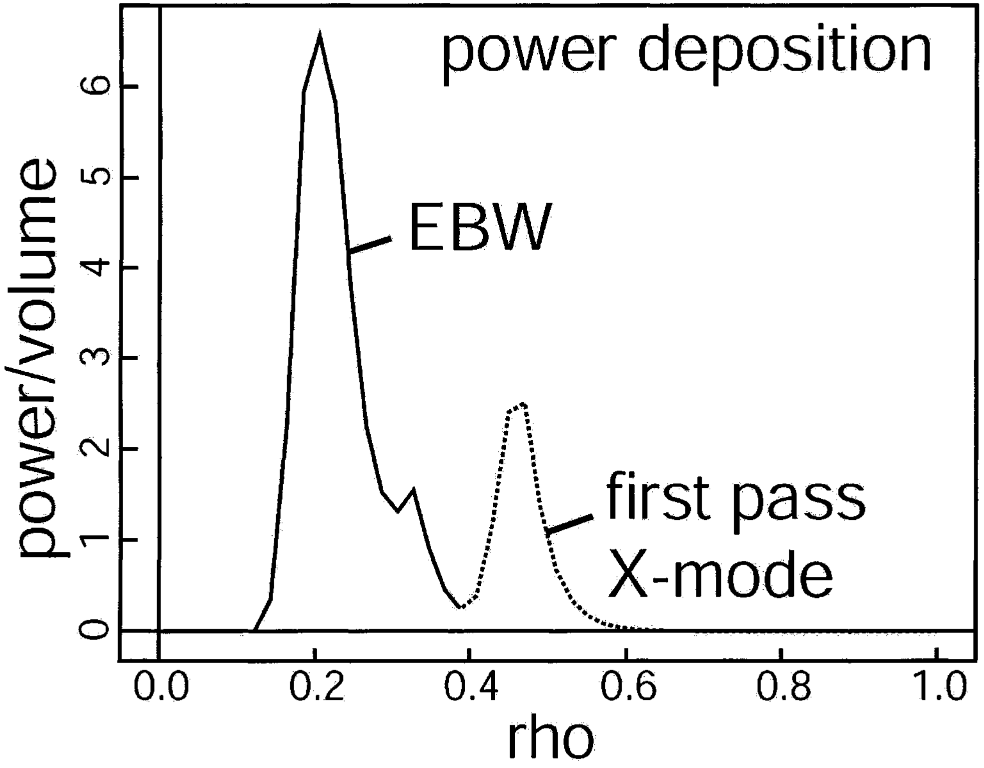

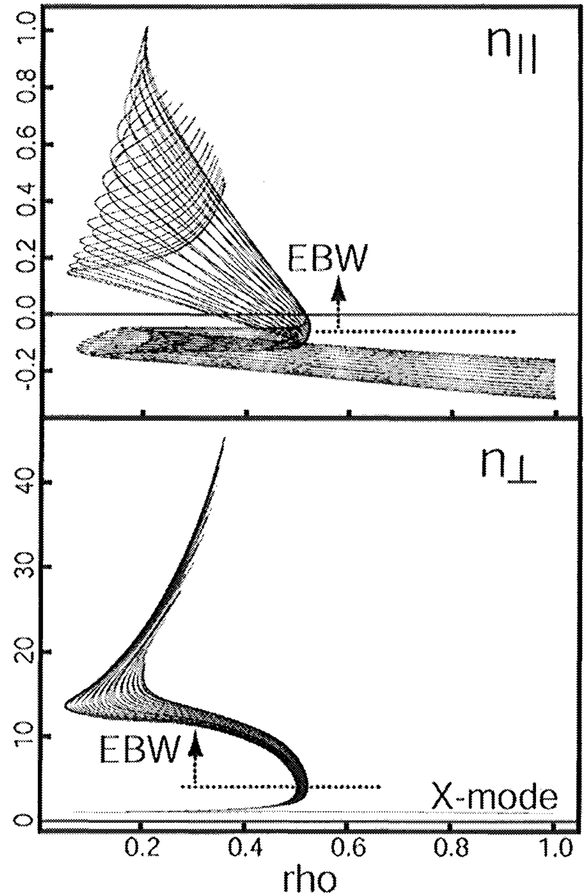

C.B. Forest, R.W. Harvey, A.P. Smirnov, Nucl. Fusion **41** 619 (2001)

Constructive interference between right and left hand cutoffs can result in efficient mode conversion

Plasma cutoffs at

$$f_L = \frac{1}{2}\left(\left(f_{ce}^2 + \frac{4f_{pe}^2}{1-N_\parallel^2}\right)^{1/2} + f_{ce}\right)$$

$$f_R = \frac{1}{2}\left(\left(f_{ce}^2 + \frac{4f_{pe}^2}{1-N_\parallel^2}\right)^{1/2} - f_{ce}\right)$$

The cold plasma resonance at $f_{uh} = \sqrt{f_{ce}^2 + f_{pe}^2}$ couples the x-mode and EBW when hot plasma effects are considered.

Cutoff-resonance-cutoff triplet can give 100 percent mode conversion:

$$C_{\max} = 4e^{-\pi\eta}\left(1 - e^{-\pi\eta}\right)$$

$$\eta = \frac{1}{\alpha}\left(\frac{\omega_{pe}L_n}{c}\right)_{uh}\left(\sqrt{1+\alpha^2} - 1\right)$$

$$\alpha = \frac{\omega_{pe}}{\Omega_{ce}}$$

Ram and Schulz, Phys. Plasmas **7** p. 00 (2001)

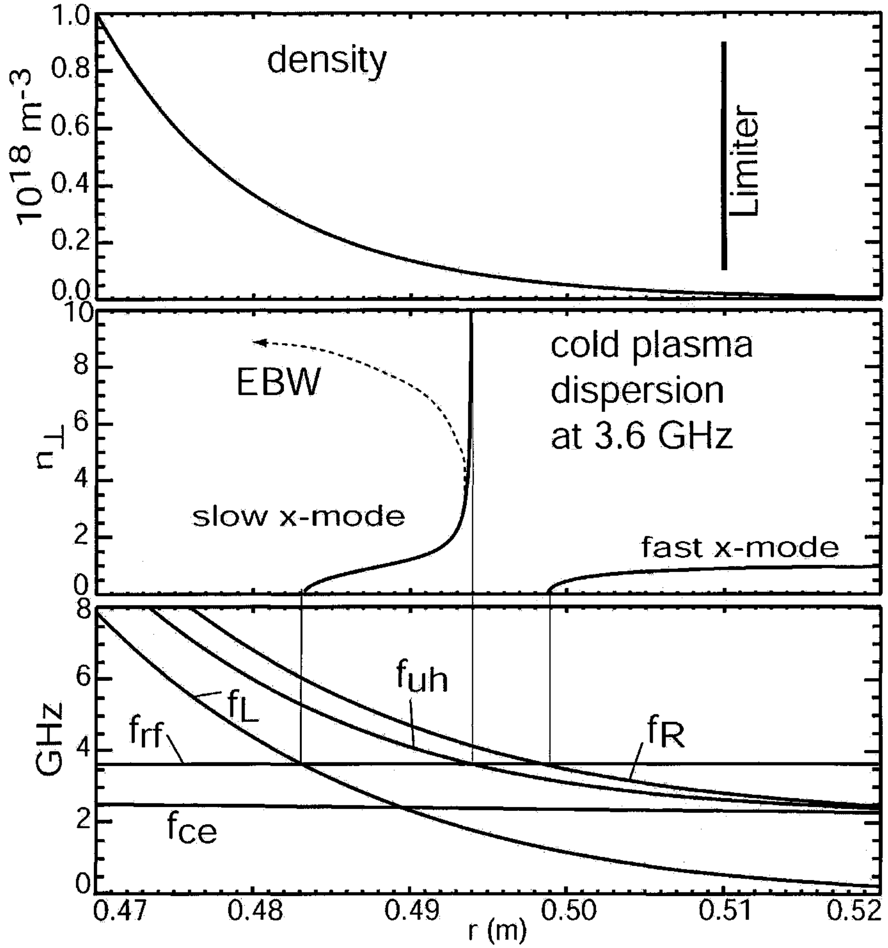

λ_{vacuum}= 9 cm

Full-wave calculations validate mode conversion process and predict surface impedance for coupling calculation

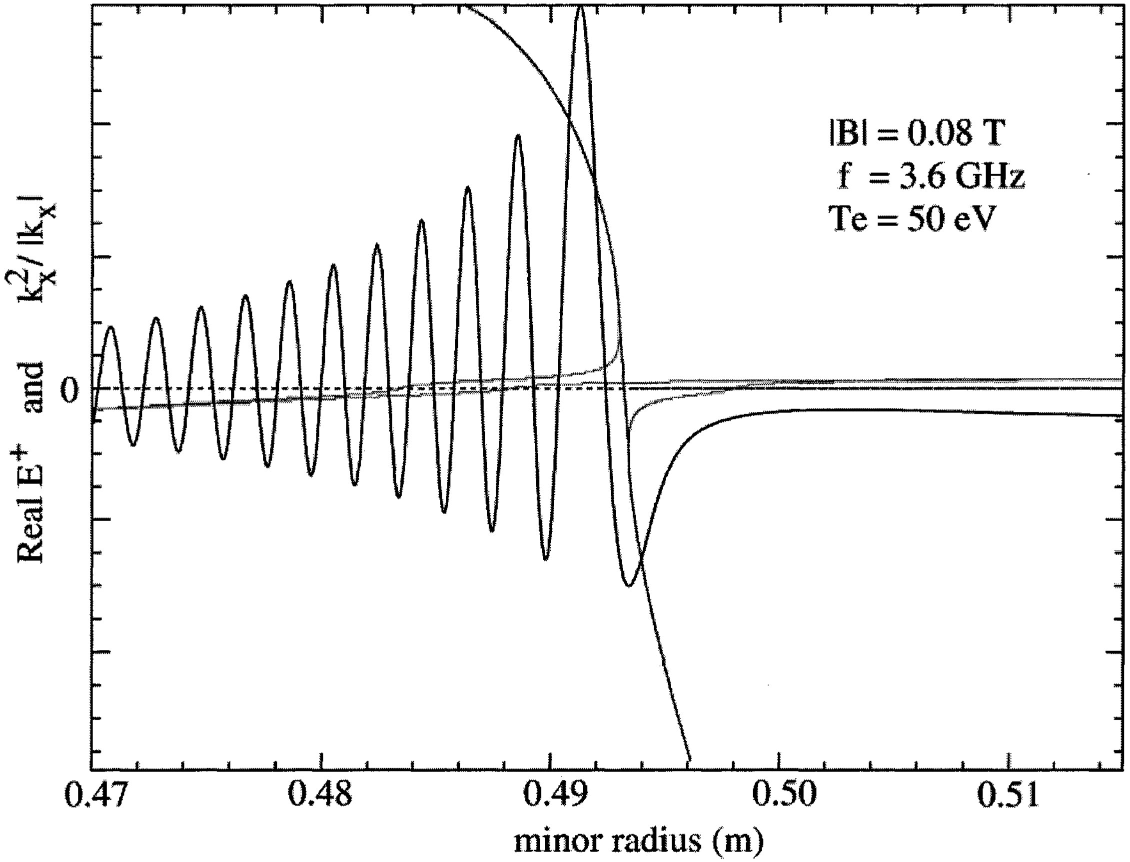

Simulations using GLOSI code, M. Carter ORNL

Impedance match depends upon density scale length and angle of incidence perpendicular launch

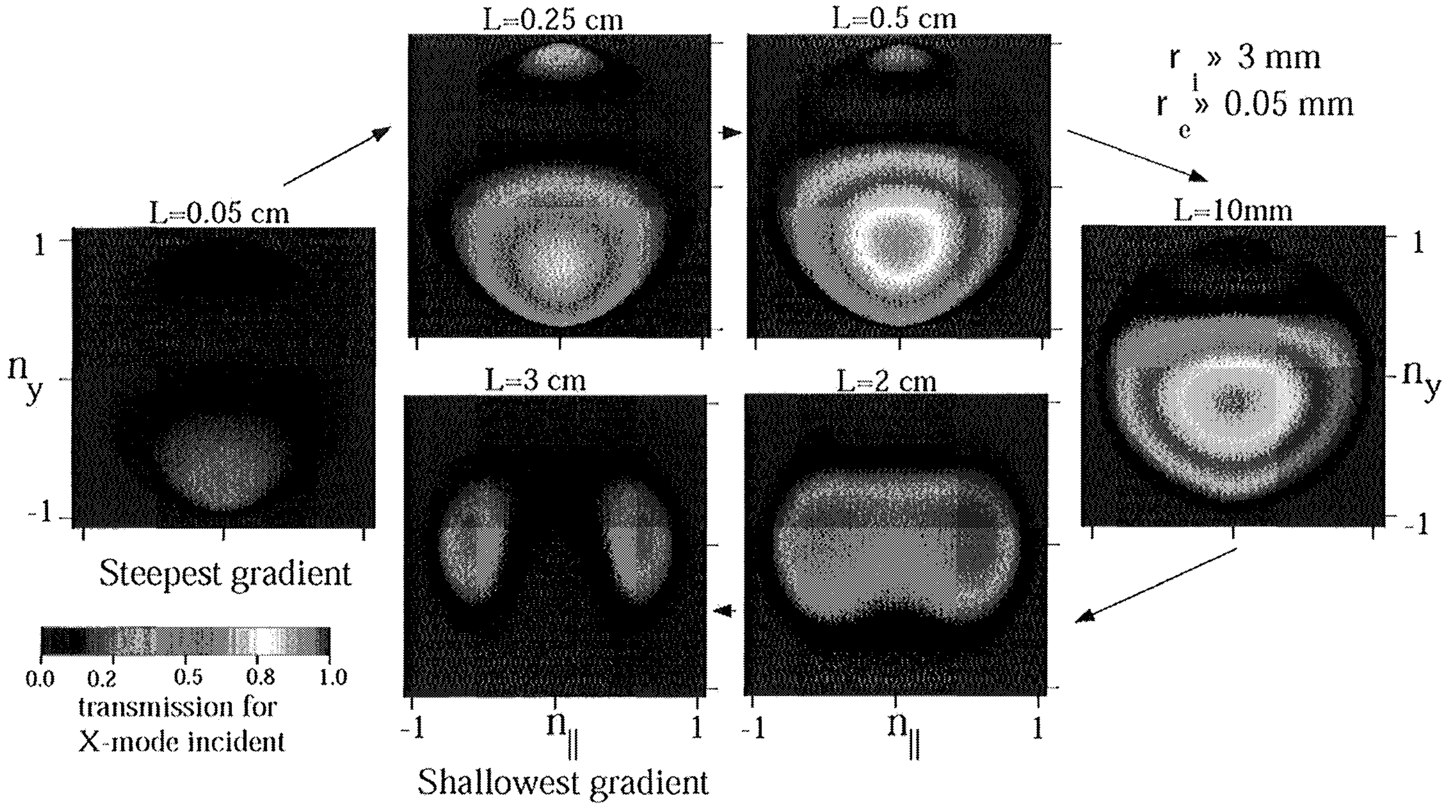

- Transmission depends on perpendicular wavenumber (n_ϕ) of incident wave
- Calculations done for a plane wave incident from vacuum

Phased array of waveguides can be used to match to EBW

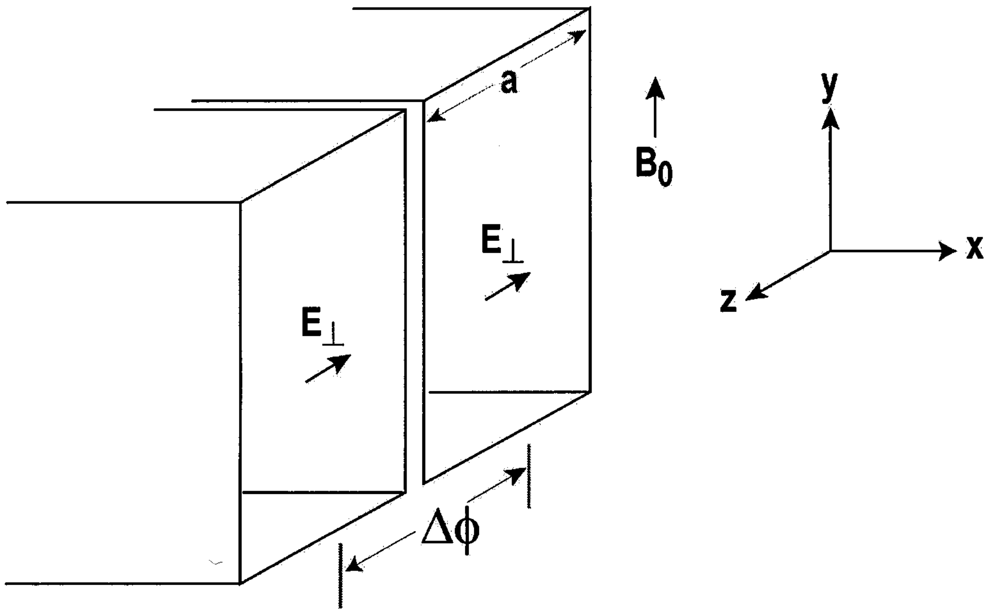

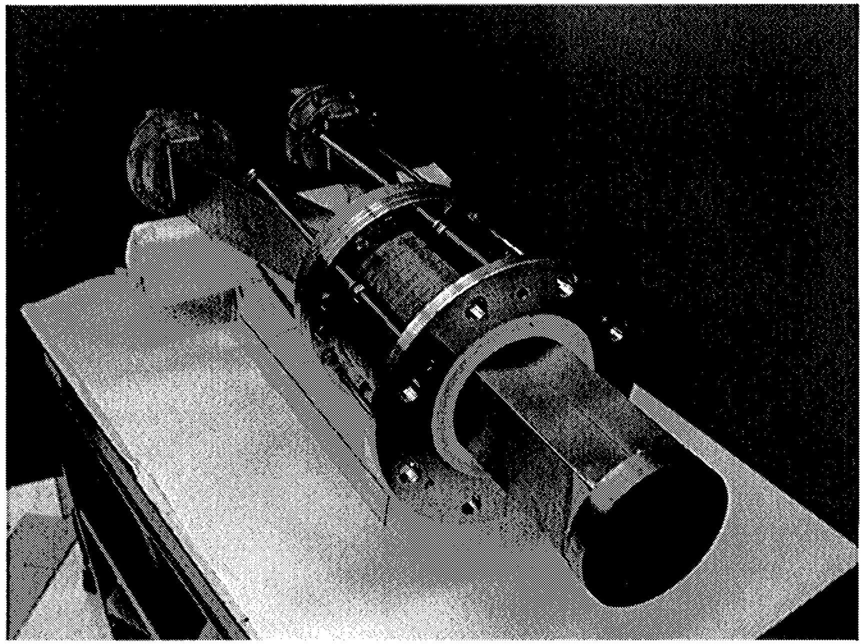

Matching E_y at $x = 0_+$and B_z in waveguide opening determines power coupled to plasma. For one waveguide

$$\frac{1-\rho}{1+\rho} \equiv \Lambda = \frac{k_o a}{2\pi\sqrt{\epsilon}} \int dn_y \mathbf{Y}(n_y) \frac{\sin^2\left(\frac{k_o a}{2} n_y\right)}{\left(\frac{k_o a}{2} n_y\right)^2} \tag{1}$$

where $\mathbf{Y}(n_y) = \left.\frac{E_y}{B_z}\right|_{x=0}$ is determined from plasma physics. Has been generalized to multiple waveguides.

[M. Brambilla, Nucl. Fusion **16** 47 (1976)]

Reflected power depends upon phase between waveguide, consistent with freespace picture

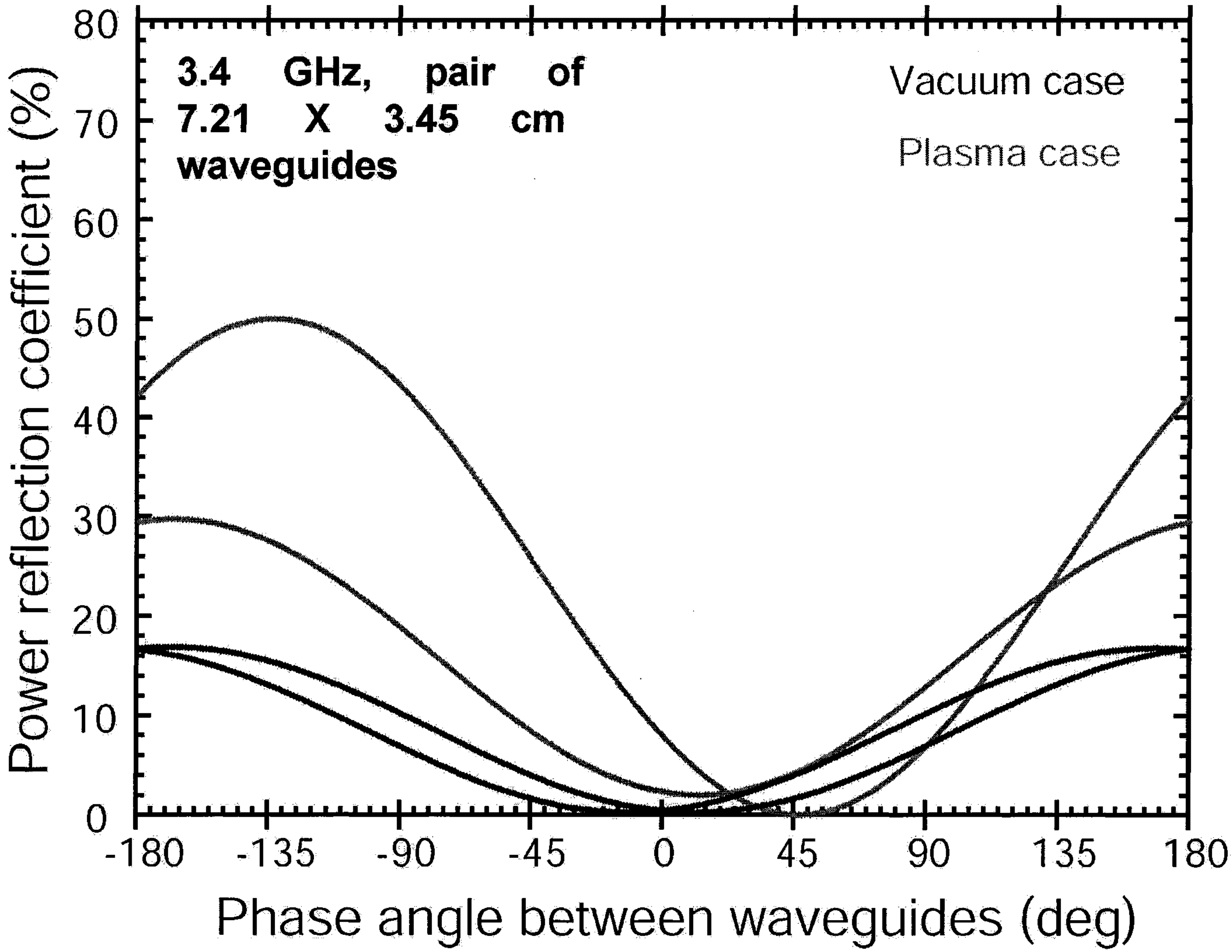

Ordinary-Extraordinary-Bernstein Mode is also possible

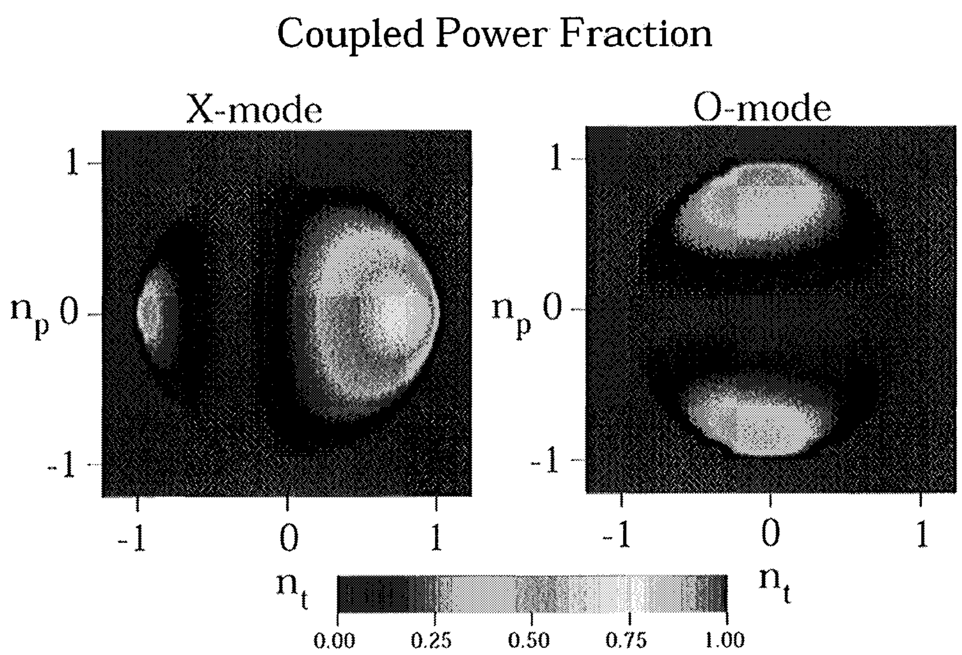

3.7-8 GHz radiometer has been constructed and absolutely calibrated

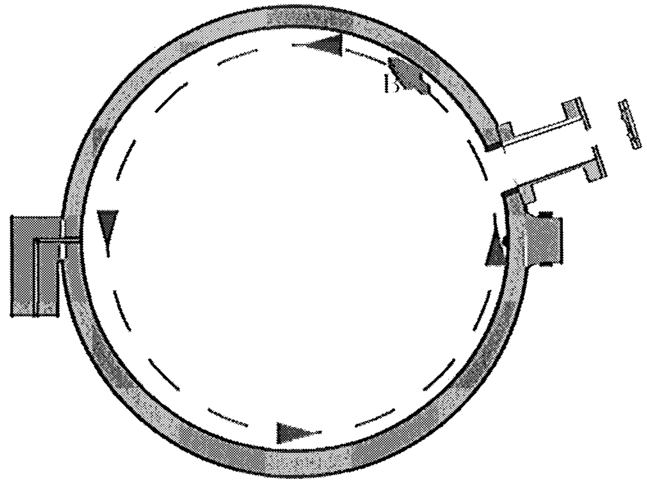

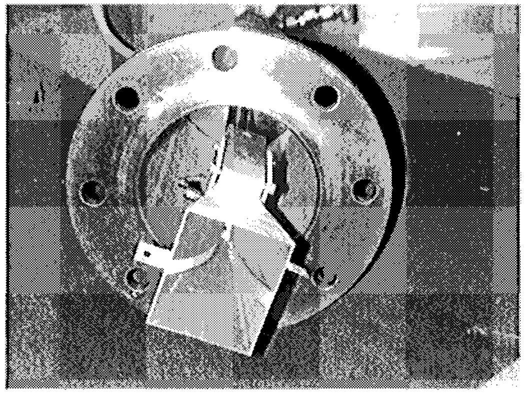

Antenna Specification

16 Channel Radiometer schematic

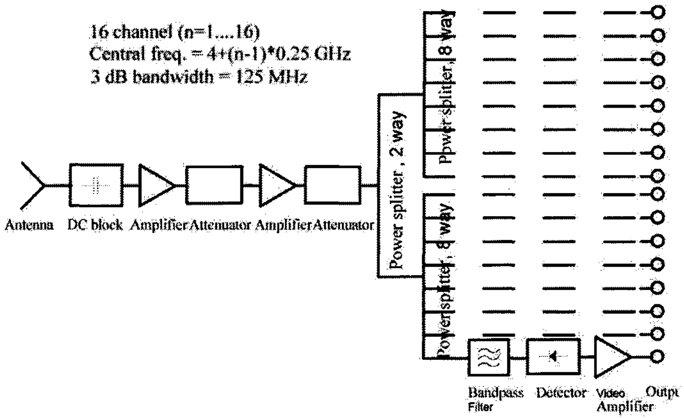

Bandwith: 3.8-8.4 GHz
Polarization: Linear
Directivity: 13-17 dB
Location: 15 deg poloidal from horizontal mid plane
Antenna looks at either O or X mode polarization.
$\Delta n_{||} = 0.5$

Emission correlates with MHD activity

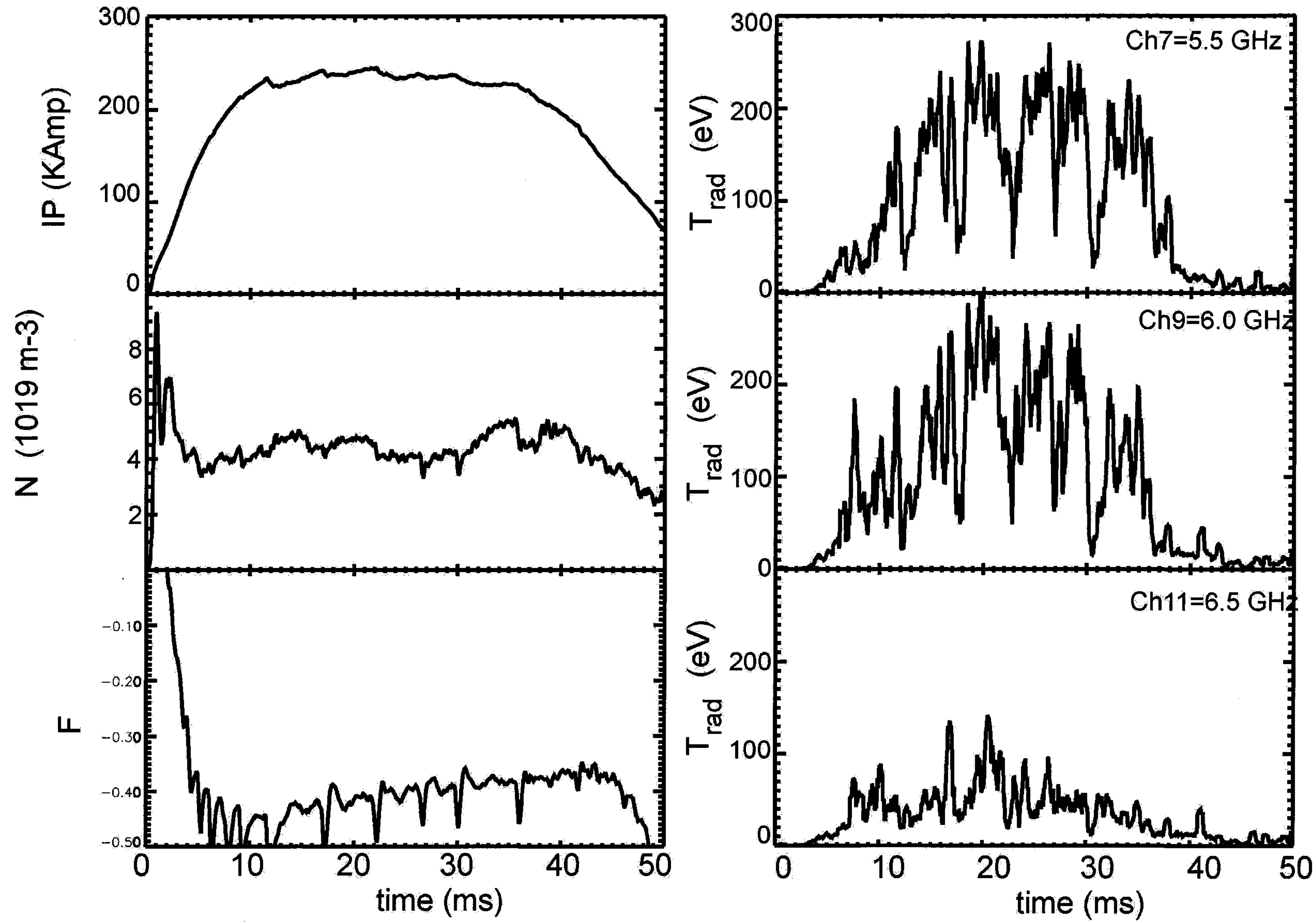

Black-body levels of electron cyclotron emission are observed

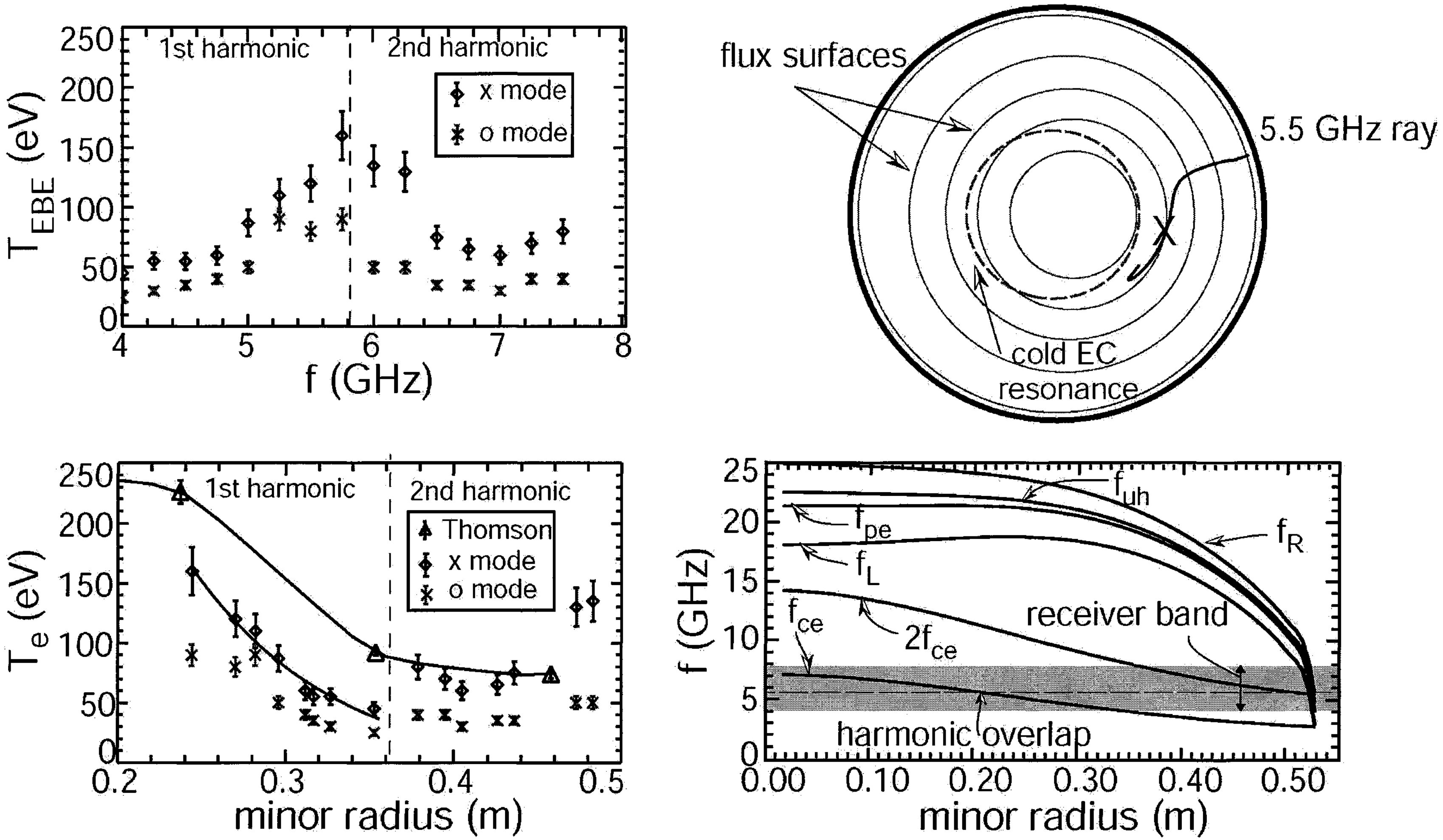

Comparison with coupling theory is underway but complicated by wall reflections

- Maximum XB mode conversion efficiency

$$C_{\mathrm{max}} = 4e^{-\pi\eta}\left(1 - e^{-\pi\eta}\right)$$

$$\eta = \frac{1}{\alpha}\left(\frac{\omega_{pe}L_n}{c}\right)_{uh}\left(\sqrt{1+\alpha^2} - 1\right)$$

$$\alpha = \frac{\omega_{pe}}{\Omega_{ce}}$$

- Applying balance of incoming radiation

$$I = I_{bb}\frac{T_{xb}}{1 - (1 - T_{xb})\,R}$$

$$T_{xb} = \frac{(1-R)\,C}{1 - RC}, \quad C = \frac{I}{I_{bb}}$$

- Reflectivity depends upon angle of incidence

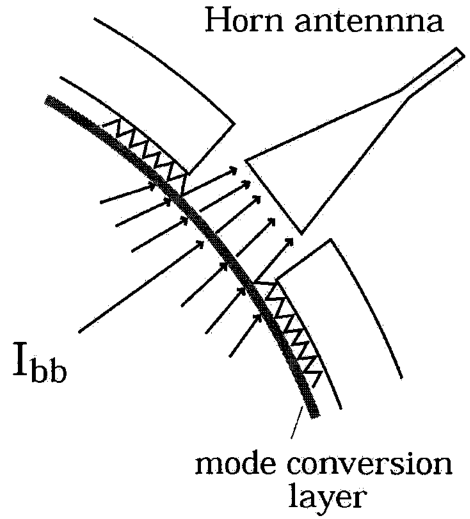

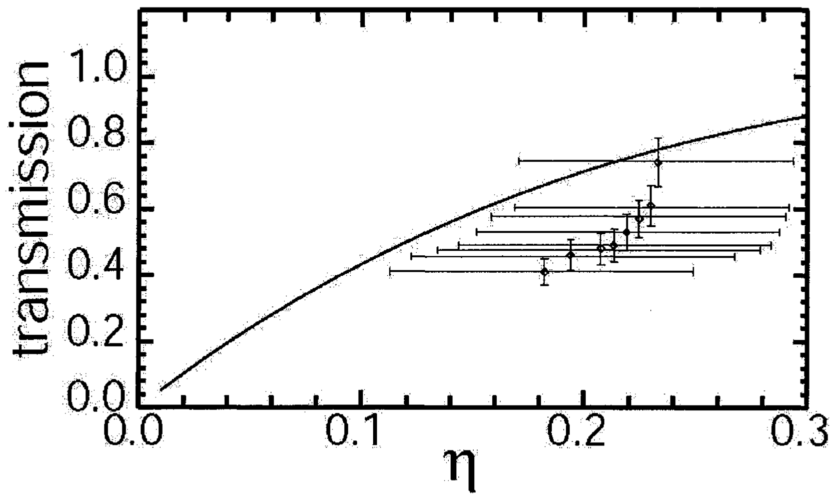

Active coupling studies are underway using single waveguide and double waveguide array

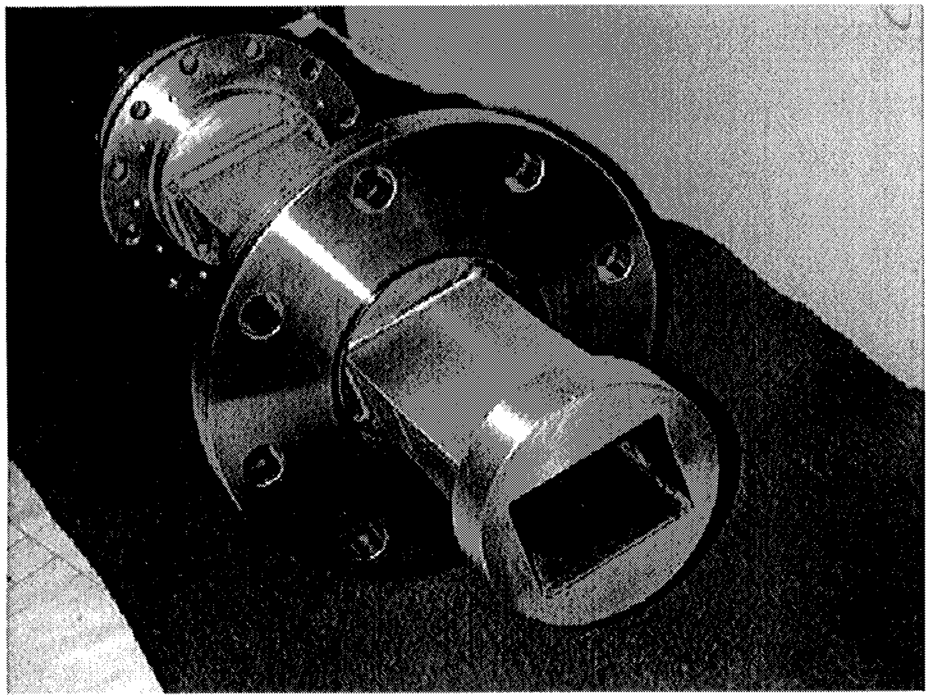

Reflectometry Schematic

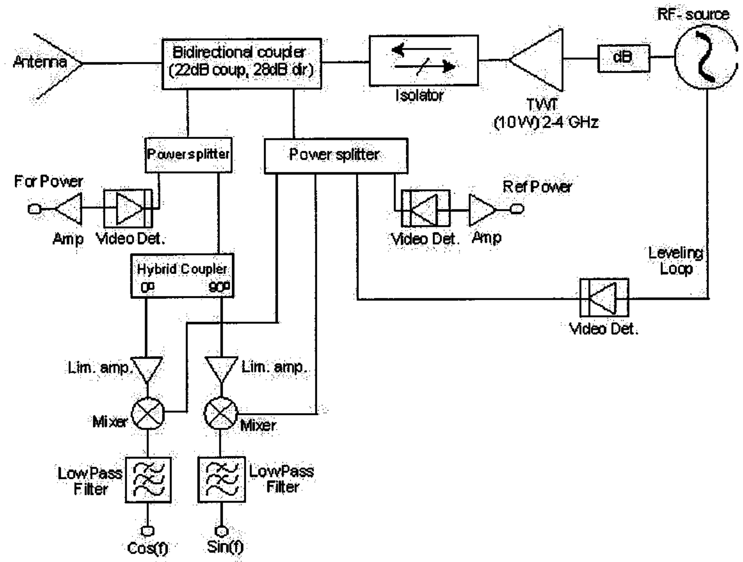

PPCD plasma presents low reflection

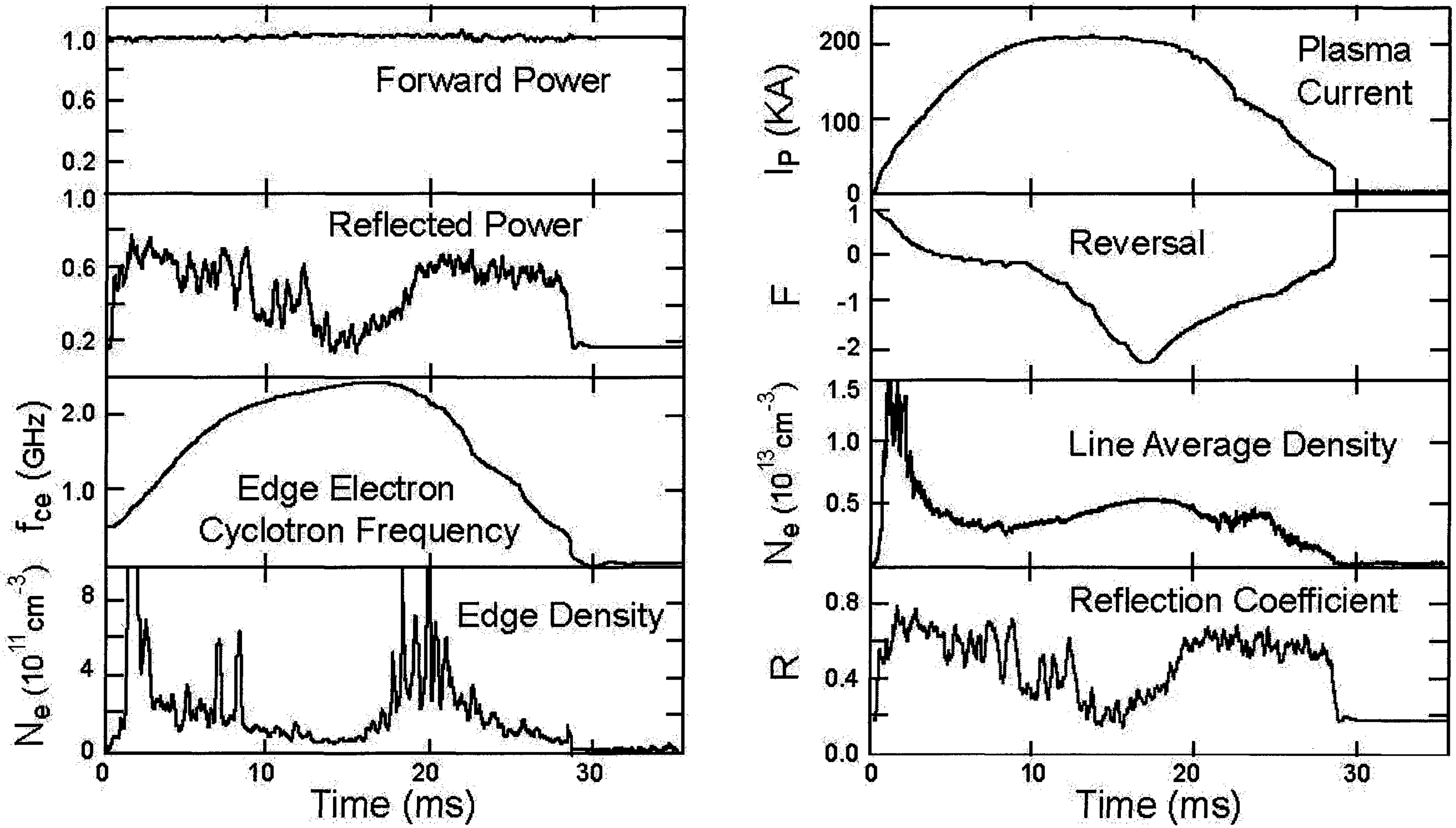

Reflection varies with frequency in accord with theory

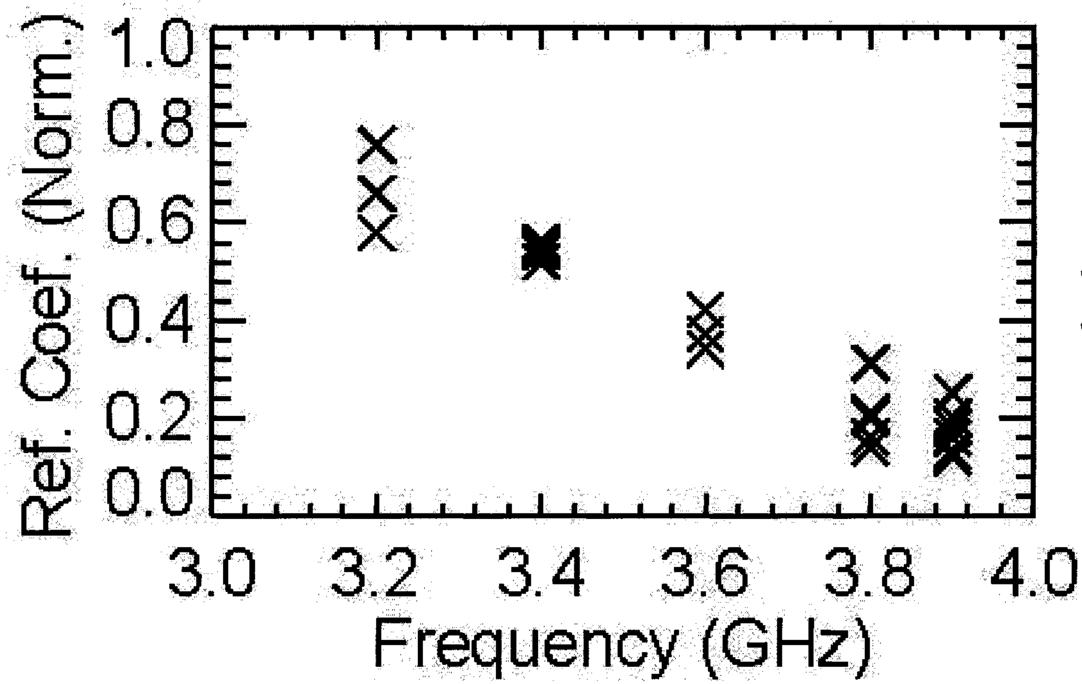

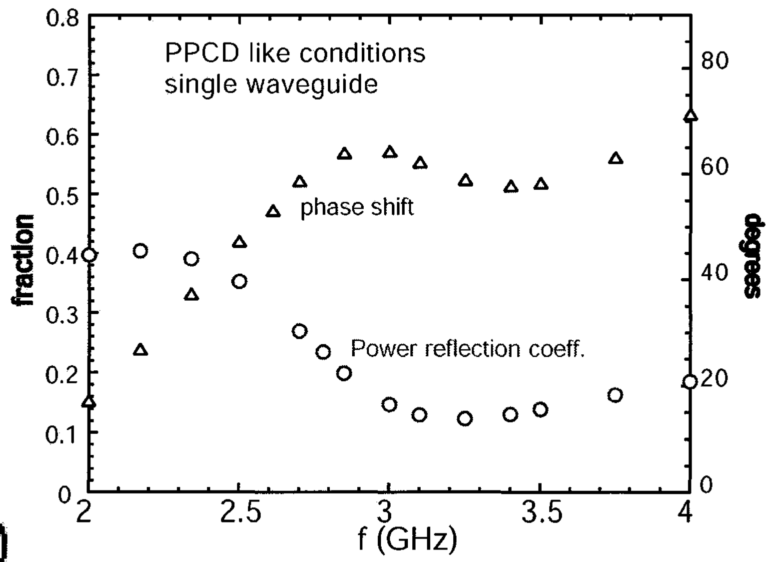

Plans for EBW

- Antenna development and edge conditioning to further optimize coupling
- Demonstrate heating
  - TWT: 3.6 GHz, 5 ms, <200 kW
  - Measure power deposition (HXR)
- Wave physics
  - Does power get to cyclotron layer in this over-dense plasma?
  - Measure EBW in plasma (probes or CO2 scattering experiment)
  - Test off-mid-plane launch CD scenario
    - N|| up-shift and hence, Doppler shifted resonance location, is different for above and below mid-plane launch (power deposition or emission region differs)